Review

A Review of Power Transfer Systems for Light Rail Vehicles: The Case for Capacitive Wireless Power Transfer

Kyle John Williams, Kade Wiseman, Sara Deilami, Graham Town * and **Foad Taghizadeh ***

School of Engineering, Macquarie University, Sydney, NSW 2109, Australia;
kyle.williams@students.mq.edu.au (K.J.W.); kade.wiseman@students.mq.edu.au (K.W.);
sara.deilami@mq.edu.au (S.D.)
* Correspondence: graham.town@mq.edu.au (G.T.); foad.taghizadeh@mq.edu.au (F.T.)

Abstract: Light rail vehicles (LRVs) are increasingly in demand to sustainably meet the transport needs of growing populations in urban centres. LRVs have commonly been powered from the grid by direct-contact overhead catenary systems (OCS); however, catenary-free direct-contact systems, such as via a "hidden rail", are popular for new installations. Wireless power transfer (WPT) is an emerging power transfer (PT) technology for e-transport with several advantages over direct contact systems, including improved aesthetics and reduced maintenance requirements; however, they are yet to be utilised in LRV systems. This paper provides a review of existing direct-contact and wireless PT technologies for LRVs, followed by an in-depth critical assessment of inductive power transfer (IPT) and capacitive power transfer (CPT) technologies for LRVs. In particular, the feasibility and advantages of CPT for powering LRVs are presented, highlighting the efficacy of CPT with respect to power transfer capability, safety, and other factors. Finally, limitations and recommendations for future works are identified.

Keywords: wireless power transfer; inductive power transfer; capacitive power transfer; light rail vehicles; power transfer systems

1. Introduction

The light rail vehicle (LRV) is an increasingly prominent component of modern urban landscapes. Since the turn of the century, LRV transport has experienced rapid growth; in 2021, over 400 cities worldwide had LRVs, with numbers increasing to meet the demand for sustainable, urban-scale transport systems [1]. Between 2015 and 2021, an average of 6.7 new systems were opened each year, with an average system rail length of over 1300 km [1], servicing over 1 billion passengers annually across the globe [2,3]. The growth is driven by city administrations endeavouring to improve air quality and streetscape aesthetics while reducing greenhouse gas emissions. With this growth in LRV use, the need for efficient, aesthetic, safe, and sustainable urban transport power systems has also become increasingly evident.

The traditional method for powering LRVs is via an overhead catenary system (OCS). OCS systems provide lower complexity and highly efficient power transfer with relatively low infrastructure costs. However, because of their high maintenance costs and the demand for cities with improved livability and mobility, OCS-free power systems are increasingly in demand.

The alimentation par sol (APS) system is a widely adopted implementation of a third rail technology developed by Alstom for their LRV group of Citadis LRVs [4]. The APS system is OCS-free as it transfers power through an energised rail (the third rail) located under the LRV bogey. Alstom's proprietary APS system operates during a safety window, whereby the section of rail in contact with the power collection arm present on the underside of the LRV is only energised while the LRV bogey is directly above that

given section of rail. Once the LRV is passed over it, the rail de-energises, while a new rail is energised forward of the previous one and takes over the powering of the LRV. The APS system is primarily used to remove the poor aesthetics of OCS. However, this system has the drawback of high installation cost and the subsequent amount of infrastructure to develop it, in comparison to OCS. Additionally, the APS system suffers from unexpected shutdowns during heaving flooding and high maintenance due to the requirement of the mechanical contact to transfer power, increasing costs over the lifespan of the development due to this needing replacement.

Wireless power transfer (WPT) is one such technology that can enable LRVs to meet the emerging requirements to improve the liveability and aesthetics in the global cities of the world. WPT technology was discovered with early experiments dating back to Nikola Tesla investigating wireless induction in the late 19th century [5]. Today WPT is, however, a newly developed technology to charge electrical devices such as vacuums, mobile phones, electric vehicles (EVs), etc. The principle of WPT lies in the foundation of transferring power through an open space (i.e., airgap) without a direct physical connection such as a cable. WPT technology is separated into two distinct categories, near field, and far field.

Near-field coupling is possible in two key modalities: inductive power transfer (IPT) and capacitive power transfer (CPT). Traditionally, IPT has been preferred for applications requiring medium power and medium distance WPT applications such as EV chargers and wireless LRV. Recent advancements in CPT technology have shown the advantages of this technology to be considered the main technological alternative to IPT. However, CPT technology requires further investigation, analysis, and validation before being introduced and applied in large-scale applications such as LRV.

While there exists a range of review papers that cover the current state of research and development into wireless power transfer technology, these review papers most commonly address IPT technology due to the existing proliferation of this research [5–7]. Other existing papers deal solely with WPT as applied to EV applications where IPT technology is again the primary focus of inquiry [8–11]. This leaves an evident lack of review into CPT for large-scale applications. However, with the increasing uptake and interest in CPT systems, few recent examples of review papers covering CPT technology exist [12–18]. These papers either present a review of WPT as applied to one specific application or a review of only recent developments, operational principles, and current limitations of CPT as a modality over the last five years. Ref. [6] provides the most comprehensive overview to date, with reference to a wide variety of applications, including transport (in the form of electric vehicles and drones). However, where the LRV application is concerned, one review of WPT technology for electric transit briefly addresses the promise of IPT for LRV application [7].

This review was motivated by a combination of recent advancements in both LRV and WPT systems and an apparent opportunity for CPT in LRV applications which has not been addressed in the literature. Furthermore, case studies of working LRV systems in the United Kingdom, the United States of America, France, Denmark, and Australia are presented and used to assess the feasibility of WPT and CPT in LRV applications.

2. Power Transfer Systems for Light Rail Vehicles

In the following section, existing LRV systems from around the world are reviewed with respect to the power transfer contact location (i.e., overhead or ground level) and assessed with respect to parameters such as safety, power transfer capability, infrastructural requirements, development timelines, cost, and efficiency.

2.1. Overhead Catenary System/Pantograph

The overhead catenary wiring system (OCS) has been the most common method of transferring power to a moving vehicle for decades. In OCS, power transfer is achieved using an external armature known as a pantograph, mounted to the roof of the train bogey that is extended to create glide contact with an overhead, current-carrying powerline,

thereby powering the train [8]. Since the pantograph and overhead cable are connected via a direct contact connection, as shown in Figure 1, OCS has a high-power transfer efficiency [9].

Figure 1. Light rail vehicle with pantograph/OCS power system. Adapted from [10] (Brecknell Willis [CC BY-SA 4.0 (https://creativecommons.org/licenses/by-sa/4.0)]).

While OCS has been widely adopted as the modality of powering a rail vehicle as it is capable of transferring power to high-speed trains and low-speed, city trams alike [8], there are some key issues with this technology. One such issue is the vibration of the train bogey and degradation in the quality of the connection to the overhead cable caused by undesirable weather conditions, leading to arcing or damage to system components [9]. Wear on the overhead cable due to continuous use conditions leads to irreversible damage to both the pantograph and overhead cable, increasing maintenance regimes, and often requiring support for 24/7 maintenance [3]. Another issue that OCS has never overcome is the aesthetic degradation of urban environments [4]. This has made powering light rail transport via alternative, less visible means a focus of local government [11]. Finally, there is the well-documented loss of life that has occurred through both misuse and malfunction of traditional OCS systems, with one case resulting in 49 deaths in Britain [12] and 14 deaths occurring in Egypt in a 4-year period [13].

2.2. Ground-Level Power Supply

The ground-level power supply, or "hidden rail" system is a power transfer method that alongside OCS, is used to power both LRV and traditional subway systems [14]. Hidden-rail is classified as a ground-level power supply, where power transfer is achieved through a ground-level connection. The most common implementation of this system is the third rail system (TRS). TRS consists of two primary components: a third rail that runs parallel to the primary rails of the track, as well as a connection/support device point on the underside of the LRV bogey [15]. In this way, a similar effect of the OCS system can be achieved, where a direct contact connection is utilised for power transfer, but with distinct advantages. TRS, due to its location and lack of exposed components, results in a more robust power transfer system [16] and one that is resistant to electromagnetic interference [3]. TRS is often cheaper to implement than OCS, due to not requiring support

frameworks and extended maintenance schedules [15,17]. Figure 2 shows a traditional implementation of TRS in the London Underground [18].

Figure 2. Third rail system in operation in the London underground adapted from [18] (Andrew Riley [CC BY-SA 4.0 (https://creativecommons.org/licenses/by-sa/4.0)]).

One major issue with most existing third rail systems is the occurrence of current leakage in the return path. The return path through the metal wheels of the train making contact with the rails [3,15], has shown relative instability historically due to stray current leaking to earth through the poorly insulated sleepers of the rails, leading to lowing of efficiency and corrosion of supporting infrastructure [3]. Furthermore, the lower voltage limitations and unavoidable gaps in service (caused by road structures) of the third rail system limit passenger loading of any train to around 60,000 passengers, per direction, per hour [3,16]. A key challenge faced by all ground-level-power-supply operated railways is the risk of flooding from heavy rains or other weather events. In one case from 2007, heavy rains in New York shut down the city's metro system for upwards of 12 h, causing significant delays and disruption [19].

2.3. Alimentation Par Sol

The APS system is the most common method of achieving power transfer for LRVs worldwide [20] and is a type of TRS. APS has proven scalability when it comes to implementation in medium-high-density urban areas where high safety, efficiency, and passenger capacity are required [20]. Furthermore, as Alstom argues, the implementation of 11-m track lengths that are automatically switched on and off based upon tram location [4,21] maximising power transfer during a "safe period" (where the tram is fully above the transfer area), greatly improves the safety of this system over OCS, and even traditional TRS. Another key feature of the APS system, that improves its reliability over traditional TRS is the ability to perform in waterlogged conditions up to 2 cm of water [4,21]. This reduces the shutdown timeline of tramways in adverse weather conditions over traditional TRS. In the case of the CBD and South-East light rail (CSELR) project in Sydney, Australia, the actual costs of developing the 12-km line reached AUD 3.1 billion [22], ballooning up from an initial budget of AUD 2.1 billion [23].

2.4. Fourth Rail System

The fourth rail system (FRS) has shown great promise in reducing stray current losses often found in TRS systems through the use of a dedicated return path, despite only three main railways adopting this technology [3]. The implementation of FRS in small areas of the London Underground as a method of improving the insulation of the return path of current, seemed to achieve promising results and as such resulted in wider adoption of this technology in the London Underground [24]. Overall, FRS is an off-shoot technology that can be associated with TRS, but has not been shown to improve efficiency greatly and is more costly to implement, but has been shown, where adopted, to decrease the effects of stray current loss in the return path of the power system [3].

2.5. Summary of Existing Power Systems

With close reference to the parameters outlined in the previous section, the advantages and challenges PT technologies are identified and summarised in Table 1.

Table 1. Summary of common power transfer systems for light rail vehicles.

Technology	Advantages	Challenges
OCS	- High efficiency - Able to support high speeds. - A high amount of power transfer enables a high capacity of passengers. - Most urban areas have existing infrastructure to support OCS.	- Requires frequent maintenance. - High infrastructure costs - Prone to issues caused by unfavourable weather conditions. - Less safe due to exposed direct contact connection
Ground-Level Power Supply (incl APS)	- Unaffected by adverse weather (bar heaving rainfall/flooding) - High efficiency - Safe for use in high-density urban areas - A robust system that requires low maintenance	- Prone to current leakage without expensive insulation or implementation of the fourth rail - Less power transfer than OCS, limiting passenger capacity and lower speed. - High initial installation cost

As a result, the challenges that a newly proposed power transfer system for LRV must overcome can be defined by the following:

- Efficiency: The system must effectively power a fully laden LRV
- Safety: The system must maintain a high level of safety when operating near pedestrian traffic
- Cost: The system must be cost effective to implement and maintain
- Reliability: The system must be robust under continuous working conditions
- Compatibility: The system must be compatible with various LRV chassis, make, model and capacity.

3. Wireless Power Transfer

WPT technology is an emerging technology that enables the transfer of electrical power through a medium other than typical metal cables or connections. Power is transmitted across a medium, such as air, using the energy of fields moving through that medium. This emerging technology has been applied to consumer electronics and healthcare devices and has shown benefits for both end-user and industrial applications and applications such as EV and LRV [25,26]. There are various existing modalities of WPT, as shown in Figure 3, that enable power transfer at various application scales.

WPT technology is separated into two distinct categories: near field and far field. Far-field applications are typically over a large distance and use a high-power electromagnetic (EM) wave to power devices [27]. This modality is best suited for very low-power applications, as the efficiency of these systems is typically very low, where only a small amount of the power is received by the target. Due to its high operating frequency (GHz–THz) and low efficiency, far-field technology is not suited for high-power applications such as EV or LRV [27]. Alternatively, there are near-field EM coupling methods, where high power transfer and small airgaps are design constraints imposed on the system [28]. Near-field coupling is divided into two key modalities: inductive and capacitive. At present, there are very few empirical comparisons into the applicability of these technologies to any given application, with [28] achieving the most detailed comparison to date as of 2015. Traditionally, IPT has been regarded as the preference for applications requiring medium power and medium distance WPT applications. However, recent advancements in CPT technology have shown great promise [29–33]. For this reason, further investigation into

the operating parameters of these technologies is required through a survey and analysis of the various existing implementations of each, especially in the last seven years. Figure 4 outlines the typical structure for any near-field WPT system, regardless of the transmitter and receiver technology.
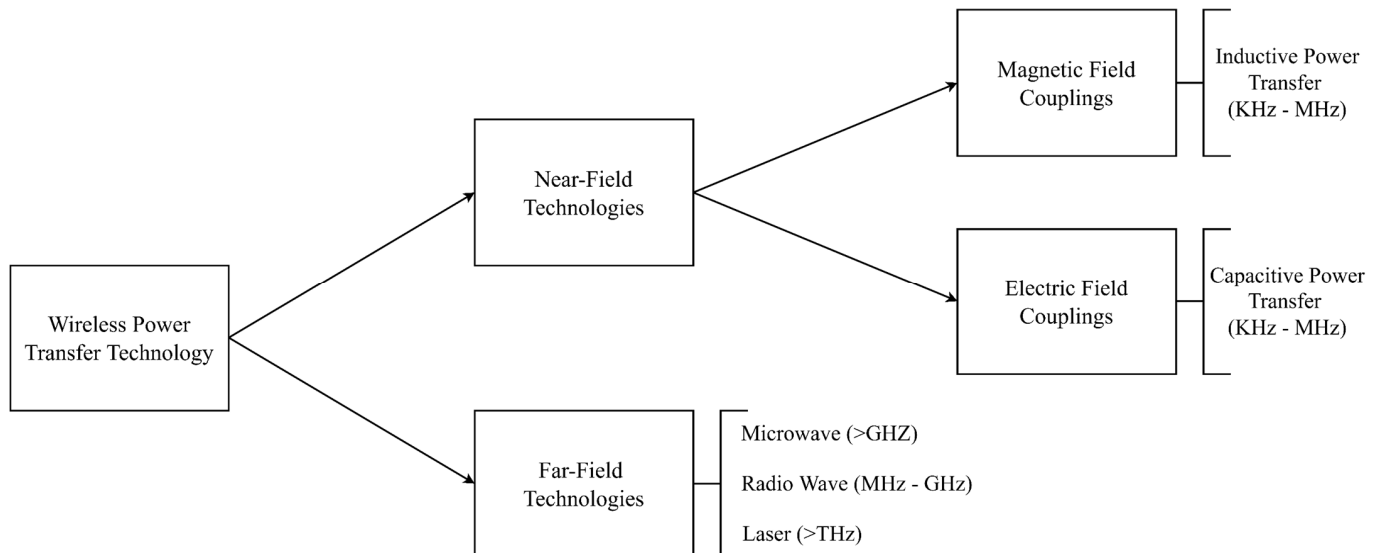

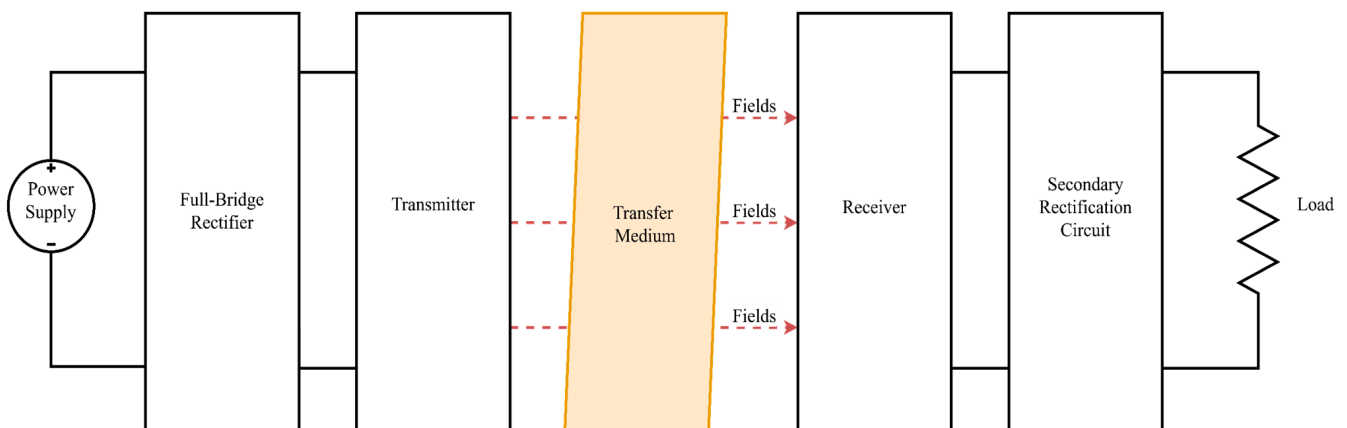**Figure 3.** Overview of the types of WPT currently in use.

Figure 4. Typical structure of WPT systems.

3.1. Inductive Power Transfer

IPT operates based upon the action of Ampere's and Faraday's laws [26]. The field generated by the current in the primary side coil is 'received' by the receiving side, and a current is induced in the secondary coil, thus allowing the transfer of power through a non-traditional medium [34]. IPT is considered a form of magnetic resonant coupling (MRC), as the compensation network made up of inductors and capacitors allows the coupling to operate at resonance, with operation in the kHz–MHz range, with power transfer tied to this frequency [35]. Figure 5 shows the operating structure of an IPT system, where the main components are shown as block elements.

While an IPT system is modelled as a typical power transformer, the construction is distinct in its lack of a shared ferrite core with primary and secondary windings attached, rather, the shared core is the medium through which fields emanate. The widespread acceptance of IPT as a means of efficiently transferring power wirelessly has caused the adoption of this technology for medical and electronic device usage in the mainstream. More recently, due to research revealing high-power transfer capability [36,37], IPT has

received much research attention for application to EV charging [38] (a charging environment not dissimilar to that of LRV). With the technology experiencing continued rapid improvement [39,40], optimisation and size reduction are now the focus of future works in this area.
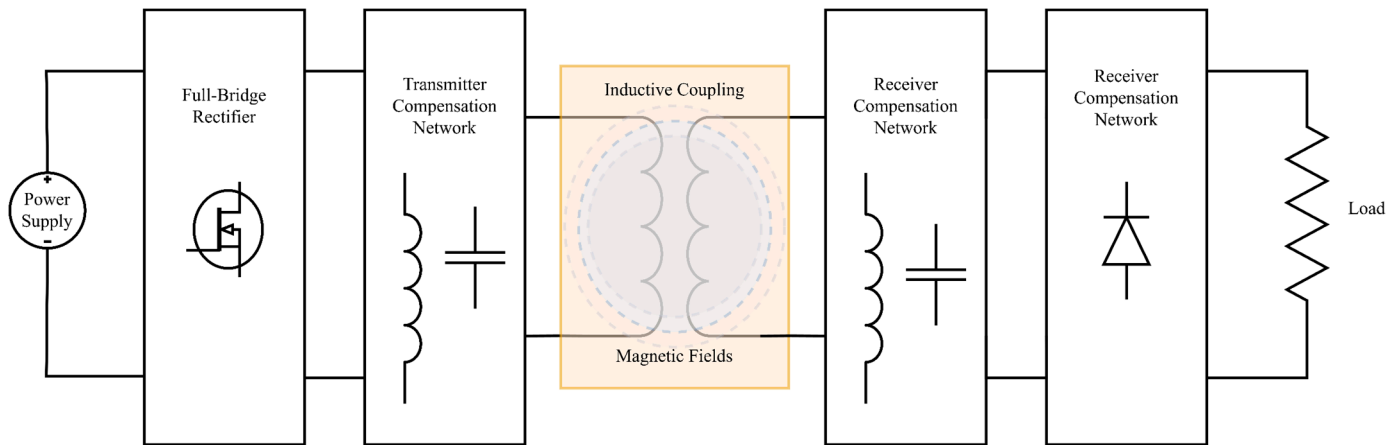

Figure 5. Typical structure of an inductive power transfer system.

3.2. Capacitive Power Transfer

CPT has experienced increasing interest over the last seven years, with PT and efficiency increasing steadily as further investigation is conducted into the viability and applicability of this emerging technology. CPT is often considered the main technological alternative (for achieving near-field WPT) to IPT [26,28,34,41]. CPT utilises high frequency (kHz to MHz) ac power to generate an electric field that allows the transfer of energy across the gap of non-traditional material (such as air) [28]. This alternating electric field generates a displacement current on the receiving side, hence achieving energy transfer [20]. The major working principle of this technology is derived from the same principles as a typical capacitor, just realised at a larger scale, where the direction of current (and thus electric field) is reversed for every half cycle of the ac operating frequency. Figure 6 shows the operating structure for a typical CPT system in block-diagram form, including the inverter, compensation network, and coupling [42].
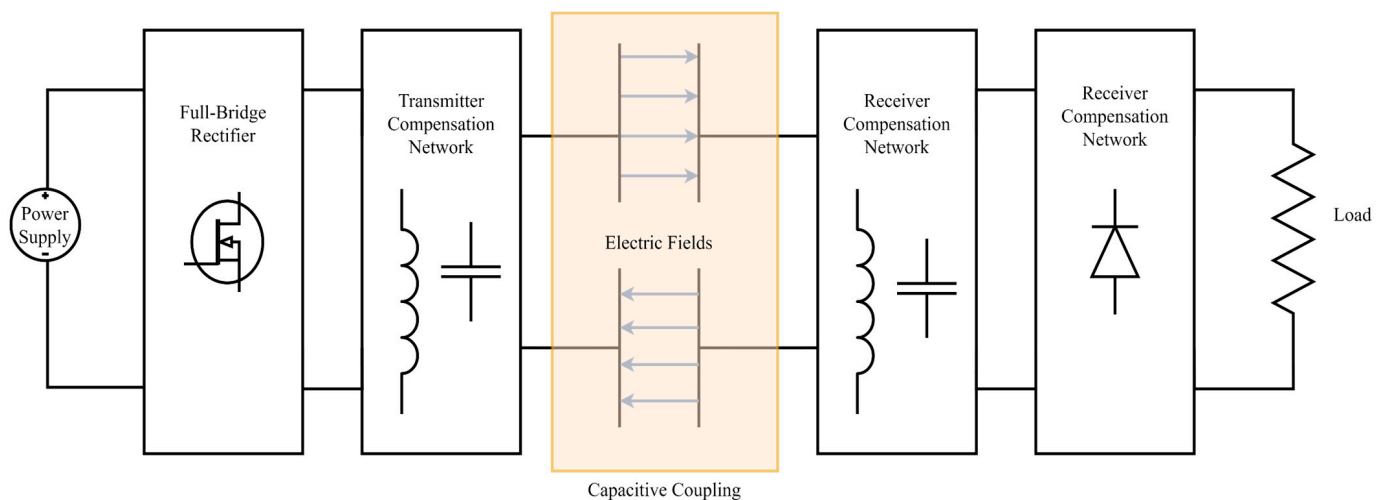

Figure 6. Typical structure of a capacitive power transfer system.

4. Comparison of Inductive and Capacitive Wireless Power Transfer Technologies

4.1. Power Transfer Capability and Efficiency

An analysis of existing CPT technology in published research revealed that multi-kilowatt power transfer ranges are common and highly possible with >90% efficiency. For LRV application, a design that achieves high power transfer density (PTD) with high efficiency is most desirable, and since compensation topology and construction type affect these parameters, these features are included for comparison. Table 2 highlights that [32,43] yielded a result of above 24 kW/m^2 with high efficiency, and [44] achieved 29.6 kW/m^2 with efficiency up to 94%. Ref. [45] achieved 51.6 kW of power transfer in experimental findings, the highest observed PTD for a CPT system to date. Ref. [46] found that a CPT coupling did not suffer performance degradation unless a foreign object is placed within 3 cm of the plates or directly in the coupling, and objects such as water or metal affect the coupler more, with a worst-case reduction in efficiency of 50%.

Table 2. Comparison of CPT systems in recent publications.

Plate Structure	Resonance Topology	Size of Plate (m^2)	Power Transfer (W)	Eff (%)	Power Density/ 1 m^2 (W)	Gap (mm)	Source
4 Plate	LCLC	0.37	2400	90.8	3243.2	150	[47]
6 Plate	LC	0.18	261	90	725.0	150	[48]
4 Plate	LC-CLC	0.42	2040	90.3	2428.6	150	[49]
6 Plate	LCL	0.37	1970	91.6	2662.2	150	[50]
4 Plate	LCLC-CL	0.0625	3000	92.46	24,000.0	40	[43]
6 Plate	CLC	0.25	2100	87.77	4200.0	150	[51]
4 Plate	CLLC	0.37	2570	89.3	3473.0	150	[52]
4 Plate	LC	0.03	1530	97.1	25,500.0	20	[32]
4 Plate	LC	0.0118	1217	74.7	51,567.8	150	[45]
2 Plate	LC	0.015	589	N/A	19,633.3	120	[53]
4 Plate	LCL	0.038	2.25	93–94	29,600.0	120	[44]
4 Plate	L	0.0375	100	87.4	2666.67	30	[54]

The research into IPT for rail applications has led to advances in the scale of prototype IPT testing in the lab. To ensure a fair comparison of true capability, technologies developed at a similar scale to those in the CPT research were examined. For instance, [37] is one such large-scale case; by utilising a 128-m transmitter, this system achieved 818 kW transfer at 82.7% efficiency using a standard "road and pickups" IPT implementation [55]. Another such industry-scale case is found in [56], where a 50-kW IPT system was tested under real tramway conditions using a mockup tram, achieving 88% efficiency even with 1000 mm misalignment in the travelling direction. The IPT implementation in [57] is a more direct comparison to existing CPT; this laboratory scale prototype achieved 5 kW of output power with 92.5%. Similarly, the findings of [58] indicate 92.5% efficiency for variable PT up to 3 kW. In practice, the PRIMOVE system by Bombardier is a real-world implementation of an IPT system for transport, capable of achieving fast 200 kW charging to an electric-bus system in Södertälje, Sweden [59]. Overall, the findings from a brief literature review of existing IPT technologies reveal high-power capability at high efficiency. Table 3 shows the tabulated findings of this IPT survey.

When considering the power transfer efficiency of an IPT coupling, the prevalence of the generation of eddy currents in nearby metal objects to an IPT coupling is critical to understanding the operational capacity of such a coupler. It has been found that as the resonant frequency of an IPT system is increased from 100 kHz to 400 kHz, eddy current losses can cause up to a 20% reduction in efficiency [60], with [61] finding a 4% reduction with the introduction of a protective metal plate. The reduction of eddy current losses is a large limiting factor for IPT.

Table 3. Comparison of IPT systems in recent publications (N/A denotes unavailable information).

Compensation Topology	Number of Coils	Power Transfer (W)	Eff (%)	Coupler Width (mm)	Gap (mm)	Source
Transformers	8	818,000	82.7	225	500	[37]
Series LC	N/A	50,000	88	600	152	[56]
H-Bridge	2	5000	92.5	N/A	5	[57]
C-C	N/A	3000	92.5	N/A	N/A	[58]
LC-LC	4	27,000	74	100	200	[39]
C-C	11	3000	90	20	N/A	[40]
LCC-LCC	2	1800	88	600	150	[62]
LCC-LCC	4	2500	N/A	400	100	[63]

4.2. Misalignment

A major identified limitation of IPT systems is the performance degradation due to misalignment between the transmitter and receiver plates [64]. Misalignment in IPT systems results in system instability, reduction of power transfer, and loss of system efficiency [64]. In IPT systems, the tolerance for misalignment is very low, with worsening performance as misalignment is increased. Ref. [65] found that with 12 cm of misalignment, efficiency drops as much as 25%. While [64] found that 3 different coupler structures experience up to 10% loss in efficiency at up to 5 cm misalignment in various directions. Another example is [66], where the mutual inductance at up to 200 mm of misalignment found that mutual inductance fell from 80 μH to as low as 5 μH at this misalignment.

In all cases in [64–66] as well as in [67], the correction of this intolerance to misalignment is achieved through the implementation of external coils to improve performance. Ref. [67] found an improvement in efficiency of 4.5% using this method. Regardless, misalignment remains a major concern for all IPT systems and requires further investigation into mitigating this effect.

The review of existing CPT systems revealed that the performance under a misalignment condition far exceeds that of IPT. While there is still a drop in efficiency in the coupling, the overall performance under a lateral or vertical misalignment is satisfactory [26,34,47]. In [47], an assessment of the lateral misalignment of a CPT coupling showed that for up to 200 mm of misalignment, there was no loss in efficiency, with a steady drop off as misalignment was increased past 250 mm. These findings agree with similar studies in [33,68], where misalignment up to 150 mm resulted in only a drop of 6% efficiency [68] and 0.5% in [33]. However, power output has been shown to decrease depending on the compensation technique. Ref. [68] indicates a large drop in power transfer performance as misalignment approaches 150 mm, whereas [33] indicated a drop of 400 W from 0 to 150 mm misalignment, while [47] highlighted a drop of 250 W.

In terms of vertical misalignment, Ref. [47] indicates a similar trend that is more drastic as the airgap is increased beyond 200 mm, with power transfer dropping steeply by 700 W. Overall, these findings agree that CPT does not face adverse effects of misalignment and is quite resistant to large misalignment cases.

4.3. External Factors and Safety

While the IPT system is capable of high-power transfer with high efficiency, it is sensitive to metal and conductive objects or debris in the air gap [55]. This causes eddy current generation on nearby metal objects [33,55], resulting in the generation of significant heat, which can cause serious safety risks and fire hazards. The key safety indicator for IPT systems limits exposure to magnetic fields [69] to a safe maximum of 205 μT (IEEE) [70] and 27 μT (ICNIRP) [71–73]. The safety of one IPT system was tested using an IPT-equipped shuttle-bus scenario where a 10 kW, 85 kHz IPT system was utilised. This exceeded the safe requirements set by the ICNIRP but was well within the IEEE recommendations [73]. Similarly, the assessment conducted in [62] revealed that for a 3.3 kW system, even in a worst-case scenario (direct lateral exposure), a human would not be exposed to fields exceeding the safe limits disclosed in [72]. However, this research does not investigate direct human exposure to the magnetic field, nor at the required level of power transfer.

Overall, exposure to magnetic fields from IPT seems to fall within a safe limit for a larger scale, vehicular application; however, care must be taken to avoid radiating magnetic fields outside WPT operating areas [26], especially in higher power transfer systems.

CPT systems utilise an electric field as the medium for power transfer and, as such, are not affected by these same limitations and challenges [50]. While increasing plate voltage is a reliable way of increasing system efficiency, t adherence to IEEE regulation C95.1-1999 [70] is of utmost importance to ensure safety. Concerns associated with electric field strength can be addressed using external metal objects and plates, such as the design in [50], that extend past the size of the coupling or material between couplers [50,74]. Findings from both [33,50] indicate significant improvement to the safe operating area by implementing this safety feature.

Another safety factor that must be considered for CPT is the risk of dielectric breakdown in the transfer medium [25,50]. This occurs at a field strength of 3 kV/mm or higher in air [25]. For systems where dielectric breakdown is a safety concern, the addition of a thin layer of Teflon [45], glass [75], or similar materials can drastically reduce this occurrence. In many instances, the voltage on the coupling plates can be limited to reduce the risk of dielectric breakdown [50]. Where field strength and human exposures are concerned, cheap and effective methods for limiting exposure to electric fields generated by CPT have proven results [43,50].

4.4. Complexity and Cost

Traditional implementation of high-frequency magnetic couplings (such as IPT systems) involves the use of Litz wire [33] to increase efficiency under the high operating frequency condition. This type of wire consists of an intertwined array of smaller wires that make up the larger wire structure [76]. This solution eliminates the skin effect as the core of the wire is not solid, and each strand of wire is insulated from the rest, thus, the overall efficiency can be increased [76,77]. However, this wire has a high manufacturing and installation cost due to the complexity of design [41,47,77].

For IPT, bulky and fragile ferrite cores are required for flux guidance that, in turn, limit the operating frequency (from core losses), leading to expensive implementation for larger scale applications where more cores are required [45]. This added complexity and cost at manufacturing is not ideal for large-scale installation in an LRV network due to the accumulation of costs and difficulties arising from requiring flux direction management systems, especially when multiple couplers are required for long track distances and high-power applications, as seen in [37].

The operating principles of CPT indicate that a capacitor can be created for an extremely low cost from easily sourced materials. The most basic implementation of a CPT coupler is two parallel sheets of a conductive metal (such as aluminium or copper), which can be acquired for low cost in large quantities [33]. Furthermore, the installation of this material requires simple manufacturing as sheet metal is already in plate form and can be easily embedded into a road surface [45], avoiding the need for large structures to support an IPT framework [26].

Overall, this makes the installation cost and complexity of the CPT solution far lower than IPT [78], making this technology highly suitable for large-scale installation. Table 4 summarises the findings of the comparison between IPT and CPT.

Table 4. Summarised conclusions of comparison between IPT and CPT.

Factor of Design	IPT	CPT
Power transfer	<800 kW	<50 kW
Efficiency	Up to 95%	Up to 95%
Performance with misalignment	Poor (<150 mm)	Excellent (<300 mm)

Table 4. *Cont.*

Factor of Design	IPT	CPT
Viable airgap distance	100–500 mm	<150 mm
Operating frequency	20 kHz–10 MHz	20 kHz–26 MHz
Safety factors	Safety risks and fire hazards due to heat generated from eddy currents, Magnetic fields around coupling at high PT, No risk of dielectric breakdown	No eddy currents, Electric fields around coupling during high PT, Risk of dielectric breakdown
Main contributing factor to losses	Losses due to eddy currents in plates and nearby objects	Losses due to low coupling between plates
Cost	High-cost materials (ferrite cores and Litz wire)	Low-cost materials (i.e., aluminium plates)

5. Capacitive Power Transfer System

5.1. Working Principles

The most basic working principle of the CPT system was briefly discussed in Section 3.2; however, a more in-depth study into the complete system operating principles is needed to understand the role of various system parameters. Figure 7 shows the most common CPT system in its entirety, with inverter/rectifier, dc source, impedance matching network, and couplers where CPT is used for the return path. CPT can also be achieved with a grounded return path replacing the return path coupler.
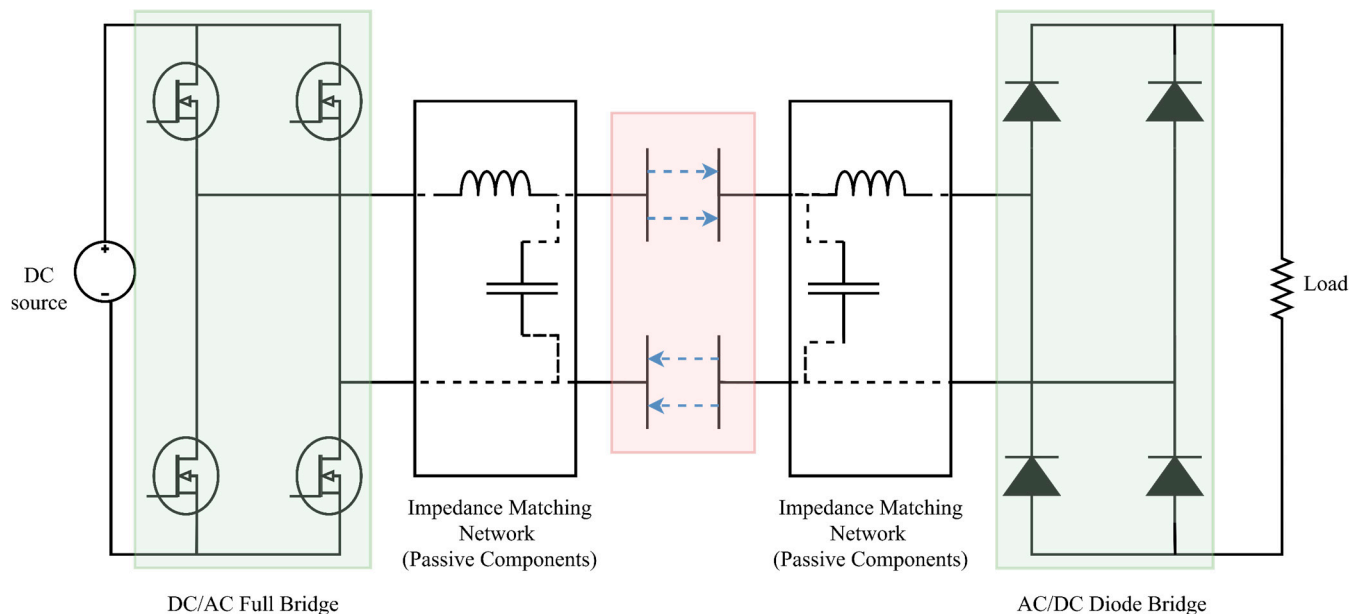

Figure 7. A complete CPT system (block diagram).

In a CPT system, power can be transferred from transmitter to receiver through an airgap and delivered to a load following rectification [79]. The operating frequency of the system follows the switching frequency of the inverter, which is closely tied to the power transfer capability of the system [80]. In a typical CPT system, the operating limits are defined by the voltage on the plates, the switching capabilities of the inverter, and the size of the plates [34,78,80]. In the following sections, a thorough analysis of the operating conditions of the CPT is conducted with close reference to parameters that must be addressed to meet the performance requirements of an LRV.

5.2. Mutual and Parasitic Capacitance Modelling

The fundamental principle of capacitance is the formation of an electric field between two metal plates. Due to this natural phenomenon, all the metal surfaces present in the

CPT changing environment will inflict a capacitance on each other that form the mutual capacitance [41,45,47,81]. The mutual capacitance is determined by the airgap distance of the coupler, the size of the coupling plates, misalignment conditions, and energy transfer direction [82,83]. Within the CPT coupling environment, any undesirable capacitances that form between adjacent plates are parasitic or internal capacitances (C14, C23, C12, and C34). Figure 8 shows this higher fidelity modelling [41,82], where a four-plate bipolar coupler is modelled as having six capacitances present. The mutual capacitance of such a system is taken at a given point between all four plates and is given by a division of main capacitances by parasitic ones.
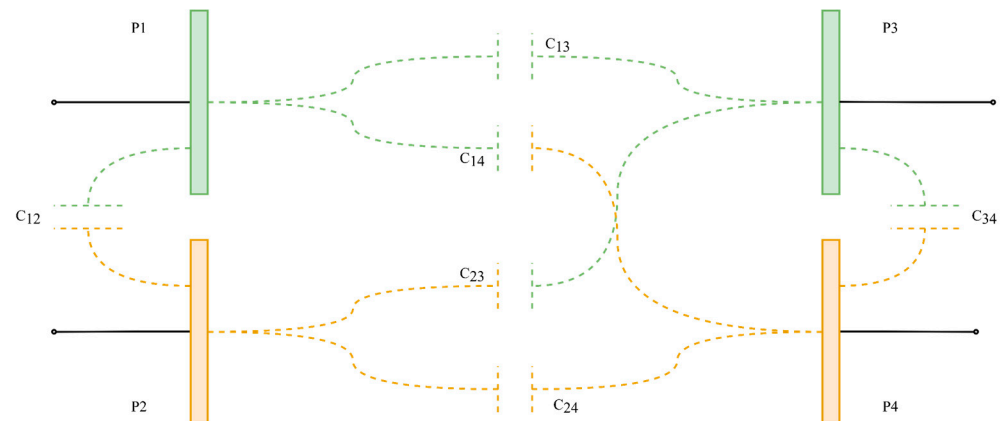

Figure 8. A complete model of the capacitances in a four-plate coupling.

While most CPT systems have parasitic capacitances in the Pico or nano-farad range [30,47,49,68,78], the accounting of these is critical in ensuring high-efficiency operation, as including these in a resonant frequency calculation is important when designing impedance matching circuits. Ref. [81] found that increasing the area of the coupling plates can also increase the mutual capacitance of the coupler in a linear relationship (mutual capacitance doubling as plate size doubled for a unipolar design).

5.3. Coupling Coefficient

The coupling coefficient is a critical numerical parameter of the CPT system that is tied directly to the efficiency of the overall system. Like in an IPT system [41], the coupling coefficient is a parameter that provides a quantitative measure of the coupling between the plates [84]. The coupling coefficient has a value that is determined by mutual and parasitic capacitances of the coupling plates, and in the case of a typical CPT system, is often in the picofarad range. As such, this parameter is directly informed by the physical size and arrangement of the coupling plates [41,68,84]. In general, the higher the coupling coefficient, the less voltage drop occurs across the coupling. In a typical CPT system as in Figure 7, a change in the coupling coefficient causes a change in the resonance frequency of the system, which leads to a change in voltage drop across the plates. When the coupling coefficient drops low enough, the voltage output can drop all the way to zero [26]. Most CPT systems developed for EV applications, or proof-of-concept designs are "loosely-coupled" CPT systems, where the coupling coefficient is very small (1–5%), with notable examples from [41,47,52,68] where the coupling plate area is under 1 m^2.

5.4. Load Value and Variation

In the EV charging environment (or LRV charging environment), the CPT coupling is often relisted as CPT plates placed in the road and on the underside of the chassis. The moving nature of the receiving plates creates a dynamic changing environment where the load varies with time [58,80]. Due to load variation, it is common for voltage ripples and power fluctuations to occur and cause increased stress on the components of the CPT system [80]. As such, the load imposed on a CPT system is a key parameter to account

for with the compensation circuit. Without this compensation, the varying load poses problems to overall system performance. Similarly, a CPT system must be designed to operate at maximum efficiency at a desired load [85]. This is because the compensation system must be tuned to enable high-efficiency power transfer at the designed load value. Incorrect load tuning can cause increasing voltage on the passive components [86] and reduced system performance [25,30,31,85,87]. A sound method for ensuring a CPT system is capable of maximum power transfer throughout load variance is proposed in [87], whereby the impedance matching circuitry is supplemented with a simple dc/dc buck-boost converter [87], allowing for accurate and effective power maximisation throughout various load values.

5.5. Voltage Phase Difference

The voltage phase angle across the coupler is the difference in phase between the voltage on the transmitting plate and the voltage on the receiving plate [30,78]. The voltage phase angle is directly responsible for the power delivered to a load through the CPT coupling at a given mutual capacitance and operating frequency, as given by (1) [78].

$$P = \omega C_M V_{p1} V_{p2} \sin \varnothing \tag{1}$$

This equation demonstrates that the transfer power (power through the coupling) is directly proportional to the operating parameters of the system (mutual capacitance, port voltages) as well as $\sin(\theta)$, where θ is the phase angle through the coupling. When the phase difference of the coupler voltages results in a low value of $\sin(\theta)$, the CPT system requires higher coupler voltages to achieve the same power delivery as a system with a value for $\sin(\theta) \approx 1$ [78]. The phase difference in the coupling is of great importance in ensuring that a given CPT can achieve high power transfer [78] under given voltage stress constraints, such as pedestrian proximity or compensation circuit limitations, and must be addressed by the compensation system design.

5.6. Imapct of Misalignment

Since power through the coupler is tied directly to the mutual capacitance of the coupling, the decrease in mutual capacitance caused by misalignment is a very important performance limitation in CPT systems [88]. An investigation into square plate plates conducted in [81] found that lateral and vertical misalignment resulted in large decreases in the mutual capacitance of the coupler, with a severe drop in performance, as lateral misalignment was increased beyond 300 mm [80]. Large misalignment conditions in a CPT system must be accounted for to ensure consistent and efficient power transfer. Similar findings indicate that disc plates exhibit higher resistance against rotational and lateral misalignment than square plates [81]. Misalignment is also tied to a change in the resonant frequency of the coupling and matching system, which in turn detunes the system and reduces system performance [88]. Since undergoing misalignment is inevitable in CPT systems, this critical component must be addressed by coupler design and impedance matching design to ensure efficiency and power transfer are maintained.

5.7. Coupler Plate Structure

The simplest structure realised for a CPT coupling is the two-plate structure, as shown in Figure 9. In this setup, there is only one receiver plate and one transmitter plate, with the return path being achieved by a typical conductive return path, such as a cable [26]. The major limitation of this design is that of the voltage on the plates since no external plates are realised in this design [70]. The two-plate design has benefits for railway applications, as the return current path can be achieved via the wheels on the metal rail track [26], thereby achieving unmatched simplicity of implementation. The two-plate structure has the advantage of simplified implementation for hardware [89] and better efficiency due to misalignment with correct compensation [68,89]. The downsized implementation of a

two-plate EV charger in [68] showed a 40 mm safety area for a 350 W CPT coupler, leaving some electric field safety concerns for full implementation.
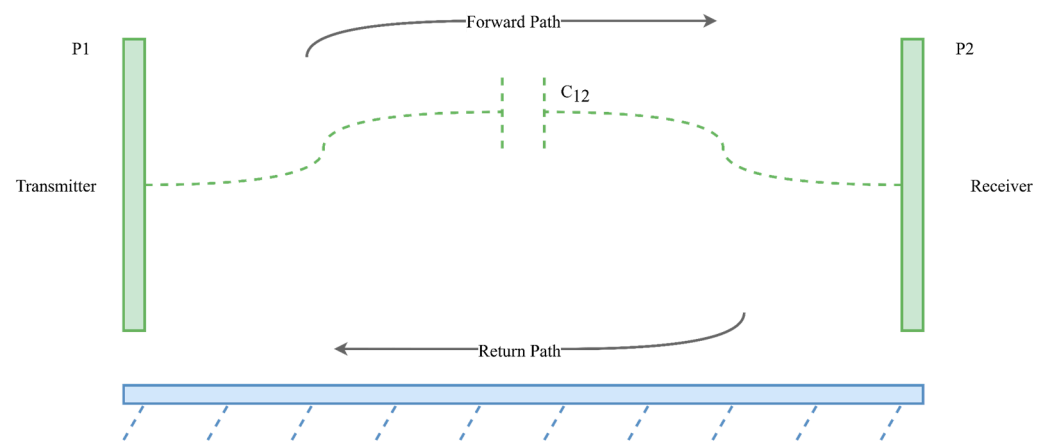

Figure 9. Two-plate bipolar coupler with conduction return path.

Another common structure for a CPT system is that of the four-plate bipolar coupler, where metal plates are placed facing each other to achieve mutual capacitance [80]. Within the bipolar structure, there are structures that have been investigated for increases in efficiency and coupling [26,80]. The row-arranged coupler (Figure 10) has two CPT couplers placed in a side-by-side configuration, where the sending and receiving plates are placed next to each other, with one coupler acting as the return path [80].
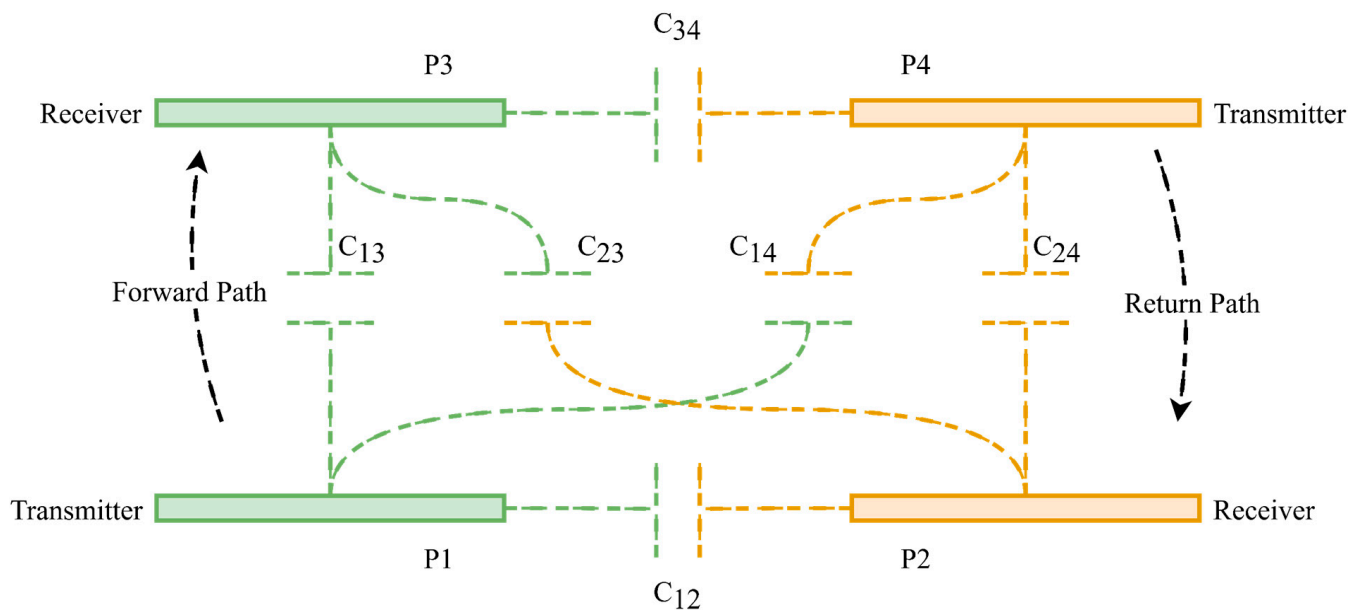

Figure 10. Row-arranged four-plate bipolar coupler.

Since parasitic capacitances arise between capacitive plates, the column-arranged coupler is proposed to improve a bipolar design by placing the plates in a column arrangement to reduce the same-plane capacitance. In the column arrangement, as shown in Figure 11, the plates are aligned centrically, allowing for a more compact implementation but with a loss in efficiency [26,80]. In general, row arrangement is desirable for its simplicity and higher efficiency.
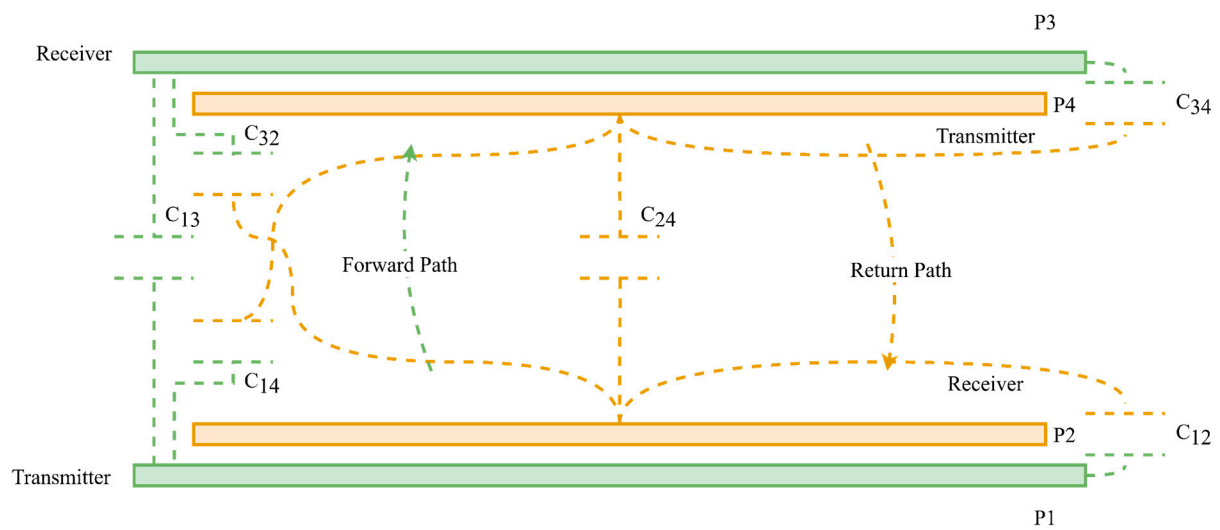
Figure 11. Column-arranged four-plate bipolar coupler.

The six-plate coupling arrangement shown in Figure 12 was originally designed to decrease the emanation of the electric field for couplings with high voltages or CPT systems designed for large PT applications [48,50]. The six-plate coupler utilises design elements of both row and column arrangements to allow the safe increase to maximum power transfer capability. The inclusion of two larger plates (P5 and P6) shields the coupling, thereby reducing the electric field strength around the coupler [50]. It should be noted that in practice, a very similar coupling type is naturally achieved in an EV or train charging environment where the underside of the car chassis or train carriage acts as the shielding plate [26,48,50]. In practice, the six-plate structure has been shown to achieve its design intention, increasing the safety of CPT by reducing the electric field emanation around the coupler. Ref. [50] found that by introducing the shielding plates above the bipolar coupling, the unsafe operating area decreases from 0.9 to 0.1 m, while [48] similarly reducing the field strength around the coupling.
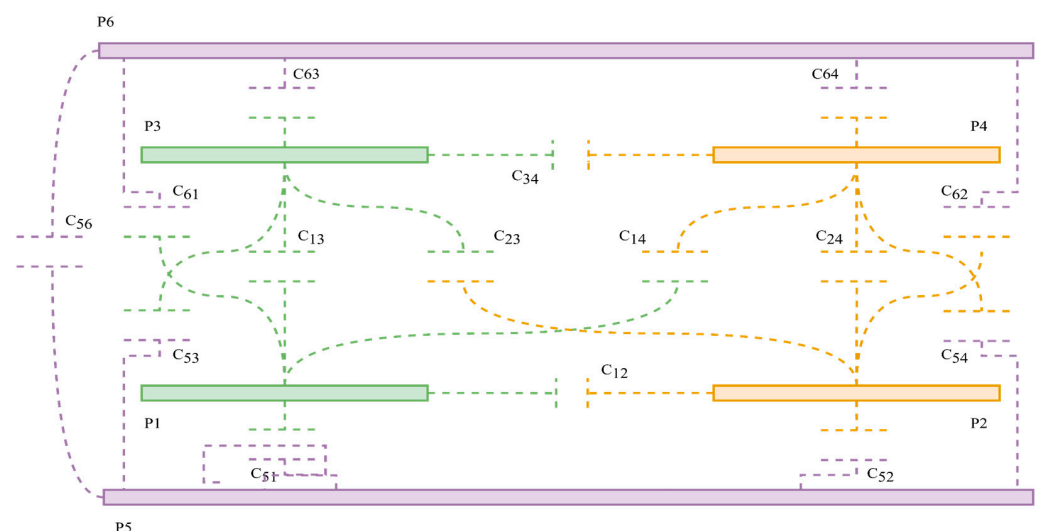

Figure 12. Structure of a six-plate CPT coupler.

In both the six-plate and four-plate bipolar structures, any misalignment of the plates causes a decrease in the capacitive coupling. The matrix structure for a CPT system, however, utilises the same receiver plate design as a bipolar coupling [26,90], but the transmitting side of the coupling is a series of plates arranged in rows or columns. The primary idea of this structure is to ensure that the misalignment position of the receiving

plates never exceeds 50% [26,90]. By utilising the transmitter made up of "m" rows and "n" columns of capacitive plates, the receiving plates can move freely above the transmitter, without experiencing diminished coupling. This concept is shown in Figure 13, where the receiving plates can move freely above a three-by-six coupler matrix [90].
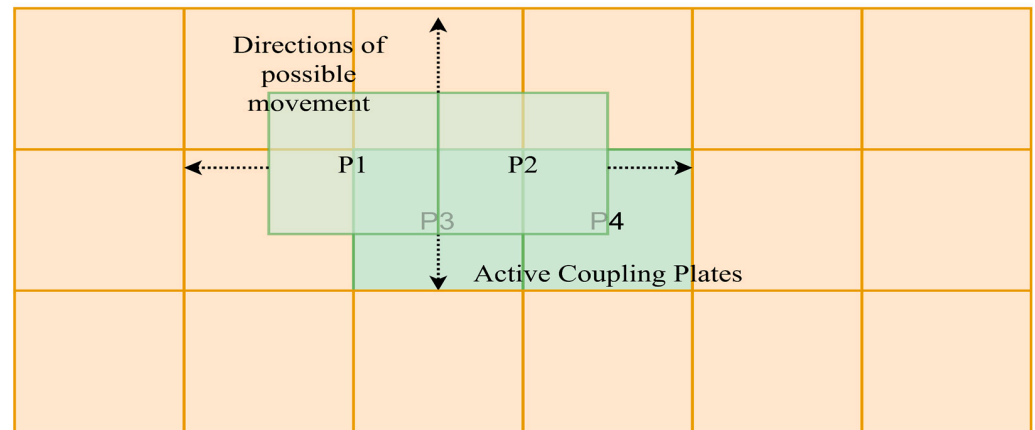

Figure 13. Matrix structure plate arrangement.

5.8. Coupler Plate Shape and Material

The most common variation of the plate shape is that of the rectangular or square coupling shape [26]. While the simplest of all coupling designs, having an area of length times width, the square or rectangular plate design has average performance in most misalignment cases [81], suffering most under rotational and lateral misalignment but performing well in a vertical misalignment case due to the large surface area of the plate. In the case of the design proposed in [81], a 500 × 320 mm rectangular plate achieved a mutual capacitance through an airgap of 100 mm of 12.79 pF. Similarly, the CPT systems in [32,43] achieved high-power transfer capability by utilising a rectangular CPT coupler. It appears from the findings in [30,41,52,68] that the chosen compensation topology for rectangular and square plates has the largest impact on the ability to achieve and maintain high efficiency under a misalignment condition. The material cost of a rectangular plate is the lowest of any implementation [26], but the cost-to-performance metric of this shape suffers due to the requirement for more materials to achieve higher mutual capacitance.

Another plate shape that has received some attention in recent research is the ring shape plate, and similarly, the disc shape. The only major difference between these structures is that the ring shape has an internal circular cut-out that is some amount smaller than the outer ring radius [26], whereas the disc is a flat piece of continuous metal with only an outer radius. The most crucial benefit of disc shape plates is the maximisation of the mutual capacitance [26,41] while reducing the effect of the skin effect present in the disc and rectangular shape [26]. This assessment agrees with the experimental findings of [45], where a disc shape coupler was utilised to achieve the highest power transfer (51.6 kW) to date in a CPT with a plate area of only 0.0118 m^2. The cost−benefit of disc shape plate is also of note, as less material is required to achieve similar mutual capacitance, allowing a higher cost-to-performance ratio over the rectangular plate shape [26]. The major drawback of a disc plate is the increased effect of misalignment. The decrease in efficiency associated with lateral and vertical misalignments is exacerbated with this shape [25] over the rectangular plate shape. However, where the vertical and rotational misalignments can be minimised, the power transfer and efficiency benefits of this shape are desirable [25,43].

Coupler material has been demonstrated to have a negligible effect on coupler performance overall, with a slight variance in voltage performance found between copper, aluminium, and zinc [91]. While copper and zinc performed the best, achieving more consistent performance with an increasing airgap, the overall effect of the performance is minimal [91]. Therefore, a cheaper metal (such as aluminium) can be used to realise a

coupling where cost is a concern, as the performance will not be a concern if the coupler has been correctly tuned and a suitable compensation system employed to manage expected misalignments [26,34].

5.9. Compensation Methods

There exist three typical methods for achieving a compensation circuit for a CPT system. The simplest of these are non-resonant systems that rely on efficient inverter technology and primarily take the form of buck-boost converters or similar structures [26,92]. This system has various limitations, the chief of which is the lack of resistance to changing physical parameters, where the system must be designed for a single airgap and plate size. Another typical topology is the use of power amplifiers constructed from resonant components to construct a resonant inverter [93]. While the physical implementation of this structure is simple, the design of this system proves difficult but can increase efficiency and allow operation up to 10 MHz without risk of detuning. The most common method for achieving compensation is the use of a high-efficiency full-bridge inverter, followed by a tuned impedance matching circuit [34]. The use of a symmetrical impedance matching circuit allows for accurate tuning [47,52], where passive components mirror each other and are designed with the same values to achieve resonance. Asymmetrical systems are particularly designed to maximise the power efficiency [41,43,49].

To ensure having a CPT system with a high-power design even under misalignment, a proper design and implementation of an impedance matching network is required [26]. The simplest impedance matching network is the LC network which includes a series inductor and a parallel capacitor [32,45,48,53]. Two inductors on both sides of the couplers maintain the balance of the voltage into and out of the coupling. The inductors resonate with the capacitors to sustain high voltages [41], while the external capacitors can increase the equivalent self-capacitance of the couplers [41], assisting the mutual capacitance to transfer power via increasing the coupling coefficient. The LC network can be designed to achieve a 90-degree phase difference between the voltages at both sides, thereby maximising power transfer across the coupling [30,41,78].

Table 5 summarises several LC circuit topologies which are reviewed and compared in [94]. The frequency bandwidth of each topology indicates the difficulty associated with correctly tuning these systems [94]. Featuring more LC circuit elements in a high-order network (such as LCLC) can improve efficiency and resistance to load variation, while adding complexity to design and implementation [94].

Table 5. Comparison of common LC resonance circuit [94].

	LC Series	CL Parallel	LC Parallel	LCL	LCLC
Frequency Bandwidth	Wide	Wide	Moderate	Narrow	Narrow
Component Stresses	Lowest	High	Low	High	Moderate
Type of Resonance	Series resonance	Parallel resonance	Parallel resonance	Parallel resonance	Parallel resonance
Complexity	Low	Low	Moderate	High	Highest

The parallel LC circuits are desirable for high-power contexts, which are achieved when a reactive component is placed in parallel with the compensated element (the coupling capacitor) [94]. Parallel resonance circuits ensure zero phase difference between the supply voltage and current (unity power factor) [47,94], while this can even be achieved with a simple LC circuit if the system is designed under the correct constraints [41,43].

Therefore LC, LCL, and LCLC are designed to increase the mutual capacitance, and therefore power transfer capacity of the coupling. Experimentally, the conclusions reached in [94] agree with the simulated findings from [95], which indicated a similar performance against misalignment gradient for LC and LCL systems, achieving up to 40% efficiency with a varying load. Ref. [95] found a drastic improvement in efficiency when using the LCLC topology; an efficiency of ~80% was achieved. A performance assessment conducted in [96] on a 6.6-kW CPT system revealed comparable results, with LC and LCL achieving almost

identical performance. Where misalignment is concerned, LC and LCL systems show tolerance to all misalignment types, with LCL offering slightly better performance [96]. LC systems have also been shown to incur higher plate voltages when high power transfer is of importance, with plate voltages being seen to increase drastically as misalignment occurs [26]. This issue is also present in some LCL systems and is completely rectified by LCLC, with the drawback of decreased misalignment performance [41]. LCLC systems were found to be more sensitive to misalignment laterally and vertically due to the finely tuned nature of the system [47,96]. Overall, the parameters and operating conditions, as well as cost and complexity constraints. indicate the most suitable option for these arrangements.

6. Feasibility of CPT for LRV Systems

6.1. Power Requirements of Existing LRV Networks

The PT system for the LRV must be able to transfer a large amount of power with high efficiency. It has been proven that CPT is capable of achieving large power transfer [32,44,45,53]; however, the ability to meet the LRV power requirement must be investigated. Various models of LRV from various global networks were investigated. In the case of an LRV network, the physical dimensions of the tram, as well as passenger capacity, vary from city to city, and as such, there are varying maximum power requirements for various LRV systems.

To verify the capability of the CPT system when applied to the LRV systems shown in Table 6, the maximum CPT power transfer density found in Section 4.1 (51.6 kW) is considered [45]. This can meet the power requirement of each LRV, while (2) can determine the amount of CPT area needed to achieve this maximum power. For compliance with IEEE Standard C95.1, a safety margin of 0.5 m needs to be applied to either side of the LRV underside area [48,50,70]. Due to the general sizing nature of this calculation, this gives a general indication of plating requirements. The underside area of the LRV bogey can be found using (3). The results of this assessment for the LRVs presented in Table 6 are presented in Table 7.

$$A_p = \frac{\text{Power Requirement (kW)}}{51.6 \text{ kW/m}^2} \tag{2}$$

$$A_b = \text{Length} \cdot (\text{Width} - (0.5 \cdot 2)) \tag{3}$$

The power requirement figure in Table 6 is derived from the maximum motor power output supplied in the technical specifications. This value acts, therefore, as a baseline power requirement, while the auxiliary power requirement is defined as a maximum of 50 kW based on the assessment of a modern LRV tram in Melbourne [97]. The power delivery method (PDM) is included to investigate the power requirements of trams with different PDMs. As the power requirements of the Alstom Citadis 305 in Sydney, Australia were not available, the power requirements were extrapolated from other similar trams within the same size and weight range (such as the Alstom Flexity series).

Table 6. Summary of critical information of existing LRV networks chosen for assessment.

LRV	Location	PDM	Length (m)	Width (m)	Max Speed (km/h)	Motor Power (kW)	Auxiliary Power (kW)	Total Power (kW)	Ref.
Bombardier Flexity 2	Blackpool, UK	OCS	32.20	2.65	70	480	50	530	[98]
Alstom Citadis 402	Paris, France	APS	42.70	2.65	60	N/A	N/A	720	[99]
Alstom Flexity Swift	Melbourne, Australia	OCS	33.45	2.65	80	510–550	50	560–600	[97]
Stadler Variobahn	Aarhus, Denmark	OCS	32.56	2.65	80	360	50	410	[100]
Brookville Liberty	Phoenix, USA	OCS/ESS	20.28	2.46	77	396	50	446	[101]
Alstom Citadis 305	Sydney, Australia	OCS/APS	33.45	2.65	80	500	50	550	

From Table 7, a minimum of 20% of the underside area of a given LRV bogey for CPT coupling material is sufficient to achieve the power requirements of a given LRV platform. This indicates a high level of feasibility when it comes to addressing LRV power requirements. For completeness, a further assessment of a worst-case scenario is conducted by assessing the maximum allowable in-rush current of the Alstom Citadis 305 LRV in use in the CSELR Sydney, Australia. In this platform, the worst-case (maximum allowable) inrush current of 1000 A is chosen to ensure the safety of service [102]. This leads to a theoretical maximum power requirement of 750 kW. Under these circumstances, the CPT system can supply the necessary power with 15 m^2 worth of capacitive plating. Overall, a CPT system capable of driving at least 51.6 kW/m^2 of power density is therefore capable of delivering the power required when the current maximum power transfer reported is transposed onto a real-world operating requirement.

Table 7. CPT coupling area requirement.

Name of LRV	Supply Voltage (VDC)	Maximum Power Requirement (kW)	Plating Area Requirement at 51.6 kW/m^2 (A_p) (m^2)	Available Underside Area (A_b) (m^2)	Req. Area of Plating on Underside (%)
Bombardier Flexity 2	600	530	10.27	53.13	19.33
Alstom Citadis 402	750	720	13.95	72.10	19.34
Alstom Flexity Swift	600	560–600	10.85–11.62	5.19	19.65–21.05
Alstom Citadis 305	750	550	10.65	55.20	19.30
Stadler Variobahn	750	410	7.94	53.72	14.78
Brookville Liberty	750	446	8.64	29.60	29.19

6.2. Structure of a CPT System for LRV

The commonly proposed method for implementing a CPT system for a moving LRV is to utilise a dynamic charging environment, where multiple transmitters are placed on the road surface [103] or in nearby structures [104,105], and the receiving plates are attached to the LRV bogey. This creates a dynamic CPT system, where the receivers are decoupled from the matching transmitters as the LRV moves, thereby allowing for the charging of the onboard battery or direct powering of the electric components [103]. This method is ideal for implementation onto an LRV, as the lack of rotational and vertical misalignment inherent in an on-rails vehicle offers increased system stability. The use of multiple transmitters or "pickups" also increases resistance to load variation [103], while the simple nature of realising this design can lower costs, as it is a simple bipolar coupling structure. The use of separate couplers rather than a long coupling also saves power and increases efficiency for single-load use cases (such as powering a single LRV) [26]. Figure 14 demonstrates the modelling of such a dynamic environment and coupling. The bipolar coupling can be further simplified by utilising a return path via metal contact of the wheels on the track, making the charging environment incur less internal capacitance while maintaining good power transfer capability.

Should the bipolar coupler be implemented in a dynamic charging environment, there will be strict size limitations for both the receiver and transmitter of the coupling. The limitations imposed on the size of the transmitters are tied to the width of the wheelbase, while the size of the receiving plates must adhere to the safety regulations and must not extend beyond the width of the LRV bogey. The systems with the greatest power transfer density of these utilise disc plates; therefore, research indicates disc plates will maintain the mutual capacitance of the coupler while lowering size requirements [26,41].

6.3. Impedance Matching Network

In practice for LRV application, the implementations of CPT that achieve the largest power transfer densities use a variation on the symmetrical LC network and were found in [32,43–45]. These systems utilise a high-fidelity model that simulates the parasitic capacitances present in a CPT coupler [32,45,45,47]. A common method of achieving this is to account for the internal capacitance of the capacitive plates using an equivalent model, as seen in Figure 15. This model includes an external capacitor and the internal

parasitic capacitances into one parallel capacitor that can be then used to calculate the resonant values for the inductors [41,47] and has been seen to enable high power transfer and efficiency [41,49,68]. This has useful implications for the complex LRV charging environment, as the parasitic capacitances present between the plates can be effectively accounted for and compensated for with the passive components of the resonance tank.
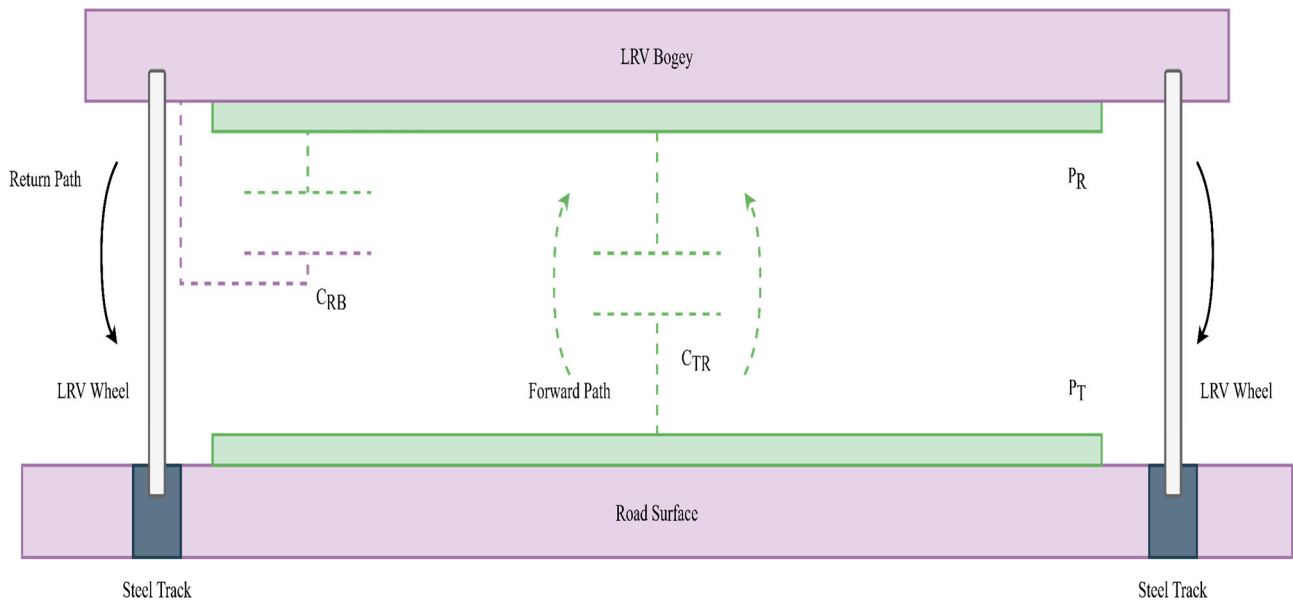

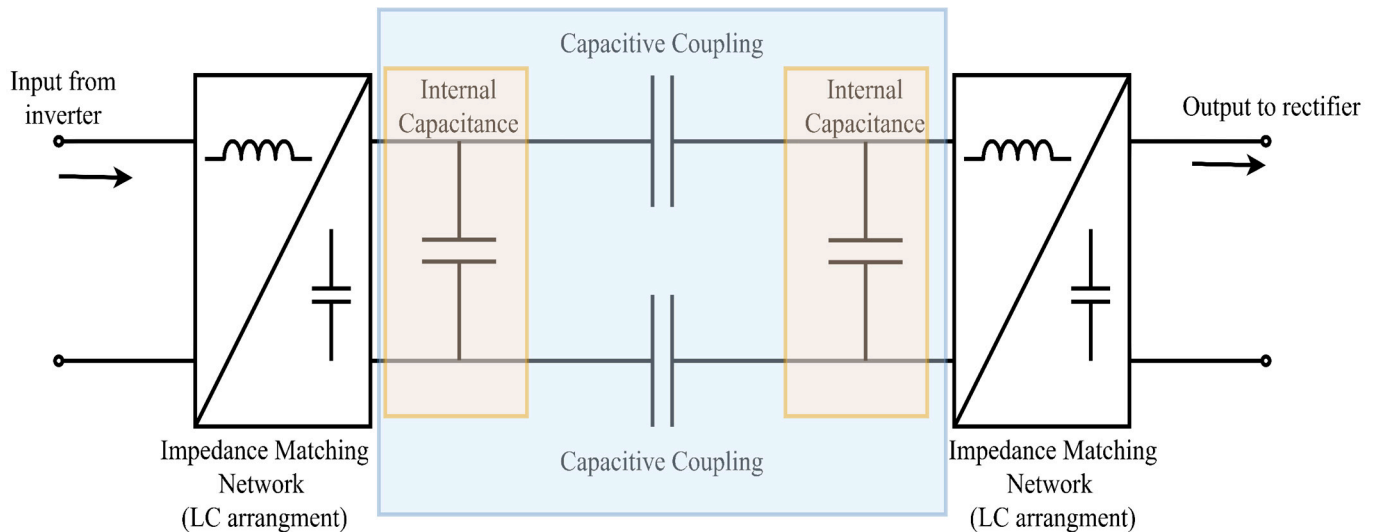**Figure 14.** LRV Environment with a two-plate structure.

Figure 15. Equivalent schematic accounting for internal capacitances.

Since the advent of GaN switches has allowed high-efficiency inverters to operate at much higher frequencies, an extremely well-tuned compensation system is able to be implemented without regard for a limitation on the operating frequency. In this case, the benefits of a well-tuned LCLC system are undeniable for increasing power transfer and system efficiency; however, the material cost and complexity involved in this tuning system cannot ensure the future scalability of the system. Since various high-power and highly efficient CPT systems have been shown to use a well-modelled LC compensation network, operating without the benefits of the LCLC systems, a double-sided LC system can achieve the requirements of the LRV−CPT system.

6.4. Safety, Other Factors, Limitations, and Recommendations

Safety is a key requirement of a power transfer system for LRV systems, as defined by IEEE C95.1. Where CPT is concerned, there are some safety concerns that must be addressed. Primarily, to ensure safe operation, the electric field around the coupling must not exceed a strength of 614 V/m at 800 kHz [70]. This safety concern must be met to ensure the safety of nearby pedestrians and LRV customers. Another concern is the risk of dielectric breakdown from the coupling plate edges to the LRV bogey and/or nearby metal objects. Refs. [32,43–45,53,105] provide examples of such couplers that can achieve high power transfer in a safe manner while maintaining high efficiency. Additionally, power electronic inverters capable of providing high power at high efficiency may need to be developed; most commercially available railway traction systems are limited to kHz switching frequencies rather than the MHz needed for CPT and WPT technologies [106].

Another safety concern requiring further attention is that of pedestrians walking on or nearby any exposed CPT plates on the road surface. If a pedestrian were to walk across an active section of LRV track and placed a foot on both the CPT surface and the return path rail, it is likely that a dangerous current could be induced in the body through capacitive coupling. This issue is like that faced by traditional TRS systems and can be addressed using switched sections of track that are only activated when the LRV bogey is overhead [4,107]. At the time of writing, no such system had been designed for CPT systems, and no to-scale prototype CPT systems had been developed.

One situation where existing power transfer systems for LRV have failed is under adverse weather conditions. For the case of water on the coupling caused by rainfall, the efficiency and power transfer of a CPT coupling are reduced [46], which may cause serious performance issues in real scenarios. Further investigation into the effects of foreign objects on CPT must also be conducted, with the development of any necessary mitigation strategies. Inundation and flooding are another concern, as CPT transmitters located underground or in natural valleys in urban infrastructure may need to be turned off to ensure safety. The development of highly efficient high-power CPT systems (or WPT systems in general) may benefit from the use of advanced computational models that facilitate rapid prototyping, developmental cycling, or incrementation. For example, artificial intelligence (AI) should not be ignored in this context, and examples of real-time applications included in [108,109] potentially have great value in the development of future CPT systems.

7. Conclusions

This paper presents a critical review and analysis of the current state of direct-contact and WPT solutions for LRV applications. Requirements for power transfer technologies in LRV applications were defined, and areas for potential improvements outlined. The most common WPT technologies, i.e., IPT and CPT, were quantitatively assessed, and their suitability for LRV applications compared with respect to power transfer capability, tolerance to misalignment, safety, cost, and the impact of external factors (e.g., weather). The comparison revealed the advantages of CPT systems in LRV applications, which were further assessed with respect to power transfer efficiency, size, weight, materials, and suitable impedance-matching networks.

The resulting meta-analysis of current LRV and CPT systems worldwide indicated that CPT should be capable of meeting the requirements of six different LRV platforms using approximately 20–30% of the underside area of the LRV. Furthermore, the inherent tolerance to misalignment makes CPT a potentially attractive PT technology for rail-based electric vehicles generally. The experimental development and demonstration of a high-power CPT system, including validation of its safety in LRV applications (e.g., in the presence of foreign objects, wet weather, etc.) is recommended for future work.

References

1. The International Assocation of Public Transport. *The Global Tram and Light Rail Landscape 2019–2021*; UITP: Brussels, Belgium, 2023.
2. Rail Unit of the UITP Secretariat. *The Global Tram and Light Rail Landscape*; International Association of Public Transport: Brussels, Belgium, 2019.
3. Abd Rahman, F.A.; Ab Kadir, M.Z.A.; Osman, M.; Amirulddin, U.A.U. Review of the AC Overhead Wires, the DC Third Rail and the DC Fourth Rail Transit Lines: Issues and Challenges. *IEEE Power Energy Soc. Sect.* **2022**, *8*, 213277–213295. [CrossRef]
4. Alstom. APS: Service-Proven Catenary-Free Tramway Operations, Alstom. 2022. Available online: https://www.alstom.com/our-solutions/infrastructure/aps-service-proven-catenary-free-tramway-operations (accessed on 27 March 2022).
5. Marincic, A.S. Nikola Tesla and the Wireless Transmission of Energy. *IEEE Trans. Power Appar. Syst.* **1982**, *10*, 4064–4068. [CrossRef]
6. Erel, M.Z.; Bayindir, K.C.; Aydemir, M.T.; Chaudhary, S.K.; Guerrero, J.M. A Comprehensive Review on Wireless Capacitive Power Transfer Technology: Fundamentals and Applications. *IEEE Access* **2021**, *10*, 3116–3143. [CrossRef]
7. Rossow, M. *Wireless Power Transfer for Electric Transit Applications*; Federal Transit Administration: Washington, DC, USA, 2014.
8. Kulkarni, S.; Pappalardo, C.M.; Shabana, A.A. Pantograph/Catenary Contact Formulations. *J. Vib. Acoust.* **2016**, *139*, 1–12. [CrossRef]
9. Kaleybar, H.J.; Brenna, M.; Foiadelli, F.; Fazel, S.S.; Zaninelli, D. Power Quality Phenomena in Electric Railway Power Supply Systems: An Exhaustive Framework and Classification. *Energies* **2020**, *13*, 6662. [CrossRef]
10. Willis, B. File:Pantograph by Brecknell Willis on a TRA EMU300 train.jpg, Brecknill Willis. 15 February 2021. Available online: https://commons.wikimedia.org/wiki/File:Pantograph_by_Brecknell_Willis_on_a_TRA_EMU300_train.jpg (accessed on 24 June 2023).
11. Cristopher English, S.Y. Sydney Light Rail Commences Revenue Service: Light Rail returns to the heart of Sydney. In *Alstom Press Release*; Alstom: Sydney, Australia, 2019.
12. Scott, R. Warning of Railway Line Dangers after 49 Die on Tracks. *BBC News*, 15 July 2010.
13. Giri, S.; Waghmode, A.; Tumram, N.K. Study of different facets of electrocution. *Egypt. J. Forensic Sci.* **2019**, *9*, 1–6. [CrossRef]
14. Bradwel, A. British Rail experience with electrical insulation. In Proceedings of the IEEE Colloquium on Mechanical Influence on Electrical Insulation Performance, London, UK, 28 February 1995.
15. Meng, H.; Wei, X.; Kang, X.; Yan, Y. Reliability Analysis of the Third Rail System Based on Fault Tree. In Proceedings of the 5th International Conference on Electromechanical Control Technology and Transportation (ICECTT), Nanchang, China, 15–17 May 2020.
16. Yadav. Traction Choices: Overhead ac vs Third Rail dc. *Int. Railw. J.* 2013. Available online: https://www.railjournal.com/in_depth/traction-choices-overhead-ac-vs-third-rail-dc/#:~:text=offering%20high%20efficiency%20%2D%20a%20750V,has%20a%20longer%20life%20expectancy (accessed on 28 March 2022).
17. White, R. C/DC railway electrification and protection. In Proceedings of the 2008 IET Professional Development course on Electric Traction Systems, Manchester, UK, 3–7 November 2008.
18. Riley, A. Conductor Rail. British Steel. Available online: https://britishsteel.co.uk/what-we-do/rail/conductor-rail/ (accessed on 30 June 2022).
19. Chan, S. Flooding Cripples Subway System. *The New York Times*. 8 August 2007. Available online: https://cityroom.blogs.nytimes.com/2007/08/08/flooding-cripples-subway-system/ (accessed on 1 April 2022).
20. Guerrieri, M. Catenary-Free Tramway Systems: Functional and Cost–Benefit. *Urban Rail Transit* **2019**, *5*, 289–309. [CrossRef]
21. Petin, B. Sydney Light Rail Project—Presentation to Stakeholders. Alstom, 28 April 2016. Available online: https://www.engineersaustralia.org.au/sites/default/files/resource-files/2017-01/sydney_light_rail.pdf (accessed on 1 April 2022).
22. Raper, A. Sydney Light Rail Budget Surpassed $3 billion, Auditor-General's Report Finds. *ABC News*, 11 June 2020.
23. Audit Office. *CBD South East Sydney Light Rail: Follow-Up Performance Audit*; Audit Office of New South Wales: Sydney, Ausrtialia, 2020.
24. Dekker, N. Stray current control-an overview of options [DC traction systems]. In *IEE Seminar on DC Traction Stray Current Control—Offer a Stray a Good Ohm?* IET: London, UK, 1999.

25. Mohammed, A.S.; Mustafa, A.Q.; Layth, A.B.; Ali, A.O.; Crăciunescu, A. A Comparative Study of Capacitive Couplers in Wireless Power Transfer. In Proceedings of the 2018 International Symposium on Fundamentals of Electrical Engineering (ISFEE), Bucharest, Romania, 1–3 November 2018.

26. Lecluyse, C.; Minnaert, B.; Kleemann, M. A Review of the Current State of Technology of Capacitive Wireless Power Transfer Technology. *Energies* **2021**, *14*, 5862. [CrossRef]

27. Belo, D.; Carvalho, N.B. 2017 11th European Conference on Antennas and Propagation (EUCAP). In Proceedings of the 2017 11th European Conference on Antennas and Propagation (EUCAP), Paris, France, 19–24 March 2017.

28. Dai, J.; Ludois, D.C. A Survey of Wireless Power Transfer and a Critical Comparison of Inductive and Capacitive Coupling for Small Gap Applications. *IEEE Trans. Power Electron.* **2015**, *30*, 6017–6029. [CrossRef]

29. Vincent, D.; Huynh, P.S.; Azeez, N.A.; Patnaik, L.; Williamson, S.S. Evolution of Hybrid Inductive and Capacitive AC Links for Wireless EV Charging—A Comparative Overview. *IEEE Trans. Transp. Electrif.* **2019**, *5*, 1060–1077. [CrossRef]

30. Wang, Y.; Zhang, H.; Lu, F. Review, Analysis, and Design of Four Basic CPT Topologies and the Application of High-Order Compensation Networks. *IEEE Trans. Power Electron.* **2022**, *37*, 6181–6193. [CrossRef]

31. Zhang, H.; Zhu, C.; Fei, L. Long-Distance and High-Power Capacitive Power Transfer based on the Double-Sided LC Compensation: Analysis and Design. In Proceedings of the 2019 IEEE Transportation Electrification Conference and Expo (ITEC), Detroit, MI, USA, 19–21 June 2019.

32. Zhang, H.; Zhu, C.; Zheng, S.; Mei, Y.; Lu, F. High Power Capacitive Power Transfer for Electric Aircraft Charging Application. In Proceedings of the 2019 IEEE National Aerospace and Electronics Conference (NAECON), Dayton, OH, USA, 15–19 July 2019.

33. Zhang, H.; Lu, F.; Hofmann, H.; Liu, W.; Mi, C.C. A Four-Plate Compact Capacitive Coupler Design and LCL-Compensated Topology for Capacitive Power Transfer in Electric Vehicle Charging Application. *IEEE Trans. Power Electron.* **2016**, *31*, 8541–8551.

34. Lu, F.; Zhang, H.; Mi, C. A Review on the Recent Development of Capacitive Wireless Power Transfer Technology. *Energies* **2017**, *10*, 1752. [CrossRef]

35. Zhang, J.; Yuan, X.; Wang, C.; He, Y. Comparative Analysis of Two-Coil and Three-Coil Structures for Wireless Power Transfer. *IEEE Trans. Power Electron.* **2016**, *32*, 341–352. [CrossRef]

36. Mahesh, A.; Chokkalingam, B.; Mihet-Popa, L. Review on Inductive Wireless Power Transfer Charging for Electric vehicles—A Review. *IEEE Access* **2021**, *1*, 99. [CrossRef]

37. Kim, J.H.; Lee, B.-S.; Lee, J.-H.; Lee, S.-H.; Park, C.-B.; Jung, S.-M.; Lee, S.-G.; Yi, K.-P. Development of 1-MW Inductive Power Transfer System for a High-Speed Train. *IEEE Trans. Ind. Electron.* **2015**, *62*, 6242–6250. [CrossRef]

38. Barsari, V.Z.; Thrimawithana, D.J.; Covic, G.A.; Kim, S. A Switchable Inductively Coupled Connector for IPT Roadway Applications. In Proceedings of the 2020 IEEE PELS Workshop on Emerging Technologies: Wireless Power Transfer (WoW), Seoul, Republic of Korea, 15–19 November 2020.

39. Huh, J.; Lee, S.W.; Lee, W.Y.; Cho, G.H.; Rim, C.T. Narrow-Width Inductive Power Transfer System for Online Electrical Vehicles. *IEEE Trans. Power Electron.* **2011**, *26*, 3666–3679. [CrossRef]

40. Ning, P.; Miller, J.M.; Onar, O.C.; White, C.P. A compact wireless charging system for electric vehicles. In Proceedings of the 2013 IEEE Energy Conversion Congress and Exposition, Denver, CO, USA, 15–19 September 2013.

41. Lu, F.; Zhang, H.; Hofmann, H.; Mi, C.C. A Double-Sided LC-Compensation Circuit for Loosely Coupled Capacitive Power Transfer. *IEEE Trans. Power Electron.* **2018**, *33*, 1633–1643. [CrossRef]

42. Chen, Y.; Zhang, H.; Park, S.-J.; Kim, D.-H. A Comparative Study of S-S and LCCL-S Compensation Topologies in Inductive Power Transfer Systems for Electric Vehicles. *Energies* **2019**, *12*, 1913. [CrossRef]

43. Liang, J.; Wu, D.; Yu, J. A Design Method of Compensation Circuit for High-Power Dynamic Capacitive Power Transfer System Considering Coupler Voltage Distribution for Railway Applications. *Electronics* **2021**, *10*, 153. [CrossRef]

44. Regensburger, B.; Kumar, A.; Sinha, S.; Xu, J.; Afridi, K.K. High-Efficiency High-Power-Transfer-Density Capacitive Wireless Power Transfer System for Electric Vehicle Charging Utilizing Semi-Toroidal Interleaved-Foil Coupled Inductors. In Proceedings of the 2019 IEEE Applied Power Electronics Conference and Exposition (APEC), Anaheim, CA, USA, 17–21 March 2019.

45. Regensburger, B.; Estrada, J.; Kumar, A.; Sinha, S.; Popvic, Z.; Afridi, K.K. High-Performance Capacitive Wireless Power Transfer System for Electric Vehicle Charging with Enhanced Coupling Plate Design. In Proceedings of the 2018 IEEE Energy Conversion Congress and Exposition (ECCE), Portland, OR, USA, 23–27 September 2018.

46. Regensburger, B.; Kumar, A.; Sinha, S.; Afridi, K.K. Impact of Foreign Objects on the Performance of Capacitive Wireless Charging Systems for Electric Vehicles. In Proceedings of the 2018 IEEE Transportation Electrification Conference and Expo (ITEC), Long Beach, CA, USA, 13–15 June 2018.

47. Lu, F.; Hofmann, H.; Mi, C. A Double-Sided LCLC-Compensated Capacitive Power Transfer System for Electric Vehicle Charging. *IEEE Trans. Power Electron.* **2015**, *30*, 6011–6014. [CrossRef]

48. Behnamfar, M.; Javadi, H.; Afjei, E. A dynamic CPT system LC Compensated with a six-plate capacitive coupler for wireless charging of electric vehicle in motion. In Proceedings of the Iranian Conference on Electrical Engineering (ICEE), Tabriz, Iran, 4–6 August 2020.

49. Lou, B.; Xu, L.; Long, T.; Xu, Y.; Mai, R.; He, Z. An LC-CLC Compensated CPT System to Achieve the Maximum Power Transfer for High Power Applications. In Proceedings of the Annual IEEE Conference on Applied Power Electronics Conference and Exposition (APEC), New Orleans, LA, USA, 15–19 March 2020.

50. Zhang, H.; Lu, F.; Hofmann, H.; Liu, W.; Mi, C.C. Six-Plate Capacitive Coupler to Reduce Electric Field Emission in Large Air-Gap Capacitive Power Transfer. *IEEE Trans. Power Electron.* **2017**, *33*, 665–675. [CrossRef]
51. Luo, B.; Mai, R.; Shi, R.; He, Z. Analysis and designed of three-phase capacitive coupled wireless power transfer for high power charging system. In Proceedings of the 2018 IEEE Applied Power Electronics Conference and Exposition (APEC), San Antonio, TX, USA, 4–8 March 2018.
52. Lu, F.; Zhang, H.; Hofmann, H.; Mi, C. A CLLC-compensated high power and large air-gap capacitive power transfer system for electric vehicle charging applications. In Proceedings of the 2016 IEEE Applied Power Electronics Conference and Exposition (APEC), Long Beach, CA, USA, 20–24 March 2016.
53. Sinha, S.; Regensburger, B.; Doubleday, K.; Kumar, A.; Pervaiz, S.; Afridi, K.K. High-power-transfer-density capacitive wireless power transfer system for electric vehicle charging. In Proceedings of the 2017 IEEE Energy Conversion Congress and Exposition (ECCE), Cincinnati, OH, USA, 1–5 October 2017.
54. Mahdi, H.; Hattori, R.; Hoff, B.; Uezu, A.; Akiyoshi, K. Design Considerations of Capacitive Power Transfer Systems. *IEEE Access* **2023**, *11*, 57806–57818. [CrossRef]
55. Chen, F.; Kringos, N. Towards new infrastructure materials for on-the-road charging. In Proceedings of the 2014 IEEE International Electric Vehicle Conference (IEVC), Florence, Italy, 17–19 December 2014.
56. Villar, I.; Garcia-Bediaga, A.; Iruretagoyena, U.; Arregi, R.; Estevez, P. Design and experimental validation of a 50kW IPT for Railway Traction Applications. In Proceedings of the 2018 IEEE Energy Conversion Congress and Exposition (ECCE), Portland, OR, USA, 23–27 September 2018.
57. Chen, L.; Nagendra, G.R.; Boys, J.T.; Covic, G.A. Double-Coupled Systems for IPT Roadway Applications. *IEEE J. Emerg. Sel. Top. Power Electron.* **2014**, *3*, 37–40. [CrossRef]
58. Nama, J.K.; Verma, A.K. An Efficient Wireless Charger for Electric Vehicle Battery Charging. In Proceedings of the 2020 IEEE 9th Power India International Conference (PIICON), Sonepat, India, 28 February–1 March 2020.
59. Schönberg, J. Bombardier's PRIMOVE Technology Enters Service on Scandinavia's First Inductively Charged Bus Line. *Bombardier*, 7 December 2016.
60. Kim, J.; Kim, H.; Kim, D.; Park, J.; Park, B.; Huh, S.; Ahn, S. Analysis of Eddy Current Loss for Wireless Power Transfer in Conductive Medium Using Z parameters Method. In Proceedings of the IEEE Wireless Power Transfer Conference, Seoul, Republic of Korea, 15–19 November 2020.
61. Yashima, Y.; Omori, H.; Morizane, T.; Nakaoka, M. Leakage Magnetic Field Reduction from New Eddy Current-based Shielding Method Wireless Power Transfer System Embedding. In Proceedings of the 2015 International Conference on Electrical Drives and Power Electronics (EDPE), The High Tatras, Slovakia, 21–23 September 2015.
62. Zhang, W.; White, J.C.; Abraham, A.M.; Mi, C.C. Loosely Coupled Transformer Structure and Interoperability Study for EV Wireless Charging Systems. *IEEE Trans. Power Electron.* **2015**, *30*, 6356–6367. [CrossRef]
63. Tran, M.T.; Thekkan, S.; Polat, H.; Tran, D.-D.; Baghdadi, M.E.; Hegazy, O. Inductive Wireless Power Transfer Systems for Low-Voltage and High-Current Electric Mobility Applications: Review and Design Example. *Energies* **2023**, *16*, 2953. [CrossRef]
64. Nutwong, S.; Sangswang, A.; Naetiladdanon, S.; Mujjalinvimut, E. Comparative Study of IPT Multi-Transmitter Coils Single-Receiver Coil System Focusing on Misalignment Tolerance and System Efficiency. In Proceedings of the 2018 21st International Conference on Electrical Machines and Systems (ICEMS), Jeju, Republic of Korea, 7–10 October 2018.
65. Sritongon, C.; Wisestherrakul, P.; Hansupho, N.; Nutwong, S.; Sangswang, A.; Naetiladdanon, S. Novel IPT Multi-Transmitter Coils with Increase Misalignment Tolerance and System Efficiency. In Proceedings of the 2018 IEEE International Symposium on Circuits and Systems (ISCAS), Florence, Italy, 27–30 May 2018.
66. Chen, Y.; Mai, R.; Zhang, Y.; Li, M.; He, Z. Improving Misalignment Tolerance for IPT System Using a Third-Coil. *IEEE Trans. Power Electron.* **2019**, *34*, 3009–3013. [CrossRef]
67. Mai, R.; Yang, B.; Chen, Y.; Yang, N.; He, Z.; Gao, S. A Misalignment Tolerant IPT System with Intermediate Coils for Constant-Current Output. *IEEE Trans. Power Electron.* **2019**, *34*, 7151–7155. [CrossRef]
68. Lu, F.; Zhang, H.; Mi, C. A Two-Plate Capacitive Wireless Power Transfer System for Electric Vehicle Charging Applications. *IEEE Trans. Power Electron.* **2018**, *33*, 964–969. [CrossRef]
69. Elekhtiar, A.; Eltagy, L.; Zamzam, T.; Massoud, A. Design of a capacitive power transfer system for charging of electric vehicles. In Proceedings of the 2018 IEEE Symposium on Computer Applications & Industrial Electronics (ISCAIE), Penang, Malaysia, 28–29 April 2018.
70. *IEEE C95.1-1995*; IEEE Standard for Safety Levels with Respect to Human Exposure to Radio Frequency Electromagnetic Fields, 3 kHz to 300 GHz. IEEE Standards Coordinating Committee: Piscataway, NJ, USA, 1999.
71. International Commission on Non-Ionizing Radiation Protection (ICNIRP). Guidelines for Limiting Exposure to Electromagnetic Fields (100 kHz to 300 GHz). *Health Phys.* **2020**, *118*, 483–524. [CrossRef]
72. International Commission on Non-Ionizing Radiation Protection (ICNIRP). Guidelines for Limiting Exposure to Time-Varying Electric and Magnetic Fields (1 Hz to 100 kHz). *Health Phys.* **2010**, *99*, 818–836. [CrossRef] [PubMed]
73. Lin, J.C. Safety of Wireless Power Transfer. *IEEE Access* **2021**, *9*, 125342–125347. [CrossRef]
74. Muharam, A.; Ahmad, S.; Hattori, R.; Hapid, A. 13.56 MHz Scalable Shielded-Capacitive Power Transfer for Electric Vehicle Wireless Charging. In Proceedings of the 2020 IEEE PELS Workshop on Emerging Technologies: Wireless Power Transfer (WoW), Seoul, Republic of Korea, 15–19 November 2020.

75. Yi, K.; Jung, J.; Lee, B.-H.; You, Y. Study on a capacitive coupling wireless power transfer with electric vehicle's dielectric substrates for charging an electric vehicle. In Proceedings of the 2017 19th European Conference on Power Electronics and Applications (EPE'17 ECCE Europe), Warsaw, Poland, 11–14 September 2017.

76. MSWire Industries. Speciality Wire—Litz Wire, MSWire. 2022. Available online: https://mwswire.com/specialty-wire/litz-wire/ (accessed on 30 April 2022).

77. Wang, W.; Zhou, L.; Eull, M.; Preindl, M. Comparison of Litz Wire and PCB Inductor Designs for Bidirectional Transformerless EV Charger with High Efficiency. In Proceedings of the 2021 IEEE Transportation Electrification Conference & Expo (ITEC), Chicago, IL, USA, 21–25 June 2021.

78. Luo, B.; Hu, A.P.; Munir, H.; Zhu, Q.; Mai, R.; He, Z. Compensation Network Design of CPT Systems for Achieving Maximum Power Transfer Under Coupling Voltage Constraints. *IEEE J. Emerg. Sel. Top. Power Electron.* **2022**, *10*, 138–148. [CrossRef]

79. Liu, C.; Hu, A.P. Steady state analysis of a capacitively coupled contactless power transfer system. In Proceedings of the 2009 IEEE Energy Conversion Congress and Exposition, San Jose, CA, USA, 20–24 September 2009.

80. Al-Saad, M.; Fadel, M.; Al-Chlaihawi, S.; Craciunescu, A. Capacitive Power Transfer for Wireless Batteries Charging. *Electroteh. Electron. Autom.* **2018**, *66*, 40–51.

81. Al-Saadi, M.; Al-Gizi, A.G.; Ahmed, S.; Craciunescu, A. Analysis of Charge Plate Configurations in Unipolar Capacitive Power Transfer System for the Electric Vehicles Batteries Charging. *Procedia Manuf.* **2019**, *32*, 418–425. [CrossRef]

82. Wang, Z.; Zhang, Y.; He, X.; Luo, B.; Mai, R. Research and Application of Capacitive Power Transfer System. *Electronics* **2022**, *11*, 1158. [CrossRef]

83. Sedehi, R.; Budgett, D.; Hu, A.P.; Mccormick, D. Effects of Conductive Tissue on Capacitive Wireless Power Transfer. In Proceedings of the WoW 2018, Montreal, QC, Canada, 3–7 June 2018.

84. Huang, L.; Hu, A. Defining the mutual coupling of capacitivepower transfer for wireless power transfer. *Electron. Lett.* **2015**, *51*, 1806–1807. [CrossRef]

85. Theodoridis, M.P. Effective Capacitive Power Transfer. *IEEE Trans. Power Electron.* **2012**, *27*, 4906–4913. [CrossRef]

86. Luo, B.; Mai, R.; Chen, Y.; Zhang, Y.; He, Z. A voltage stress optimization method of capacitive power transfer charging system. In Proceedings of the 2017 IEEE Applied Power Electronics Conference and Exposition (APEC), Tampa, FL, USA, 26–30 March 2017.

87. Bui, D.; Mostafa, T.M.; Hu, A.P.; Hattori, R. DC-DC Converter Based Impedance Matching for Maximum Power Transfer of CPT System with High Efficiency. In Proceedings of the 2018 IEEE PELS Workshop on Emerging Technologies: Wireless Power Transfer (Wow), Montreal, QC, Canada, 3–7 June 2018.

88. Qing, X.; Su, Y.; Hu, A.P.; Dai, X.; Liu, Z. Dual-loop Control Method for CPT System under Coupling Misalignments and Load Variations. *IEEE J. Emerg. Sel. Top. Power Electron.* **2021**, *10*, 4902–4912. [CrossRef]

89. Zou, L.J.; Hu, A.P.; Su, Y.-G. A single-wire capacitive power transfer system with large coupling alignment tolerance. In Proceedings of the 2017 IEEE PELS Workshop on Emerging Technologies: Wireless Power Transfer (WoW), Chongqing, China, 20–22 May 2017.

90. Liu, C.; Hu, A.P.; Dai, X. A contactless power transfer system with capacitively coupled matrix pad. In Proceedings of the 2011 IEEE Energy Conversion Congress and Exposition, Pheonix, AZ, USA, 17–22 September 2011.

91. FRahman, K.A.; Saat, S.; Khafe, A.; Yusop, Y.; Husin, S.H.; Jamaluddin, M.H. Efficiency comparison of capacitive wireless power transfer for different materials. *Int. J. Power Electron. Drive Syst. IJPEDS* **2020**, *11*, 200–212.

92. Ge, B.; Ludois, D.C.; Perez, R. The use of dielectric coatings in capacitive power transfer systems. In Proceedings of the 2014 IEEE Energy Conversion Congress and Exposition (ECCE), Pittsburgh, PA, USA, 14–18 September 2014.

93. Choi, J.; Tsukiyama, D.; Tsuruda, Y.; Davila, J.M.R. High-Frequency, High-Power Resonant Inverter With eGaN FET for Wireless Power Transfer. *IEEE Trans. Power Electron.* **2018**, *33*, 1890–1896. [CrossRef]

94. Yu, S.-Y.; Chen, R.; Viswanathan, A. Survey of Resonant Converter Topologies. In *Power Supply Design Seminar*; Texas Instruments Incorporated: Dallas, TX, USA, 2018.

95. Kodeeswaran, S.; Gayathri, M.N. Performance Investigation of Capacitive Wireless Charging Topologies for Electric Vehicles. In Proceedings of the 2021 International Conference on Innovative Trends in Information Technology (ICITIIT), Kottayam, India, 11–12 February 2021.

96. Al-Saadi, M.; Hussien, E.A.; Ahmed, S.; Craciunescu, A. Comparative Study of Compensation Circuit Topologies in 6.6 kW Capacitive Power Transfer System. In Proceedings of the 2019 11th International Symposium on Advanced Topics in Electrical Engineering (ATEE), Bucharest, Romania, 28–30 March 2019.

97. Anderson, D.E.; Croset, A. *New Traction Power Technologies to Improve the Melbourne Tram Network*; Department of Transport Victoria: Melbourne, Austrialia, 2019.

98. Gebauer, H. *Flexity 2 Tram*; Bombardier: Vienna, Austria, 2012.

99. Alstom. *Rolling Stock Tramway Citadis Marchaux—Paris Citadis Line T3*; Alstom: Montreal, QC, Canada, 2012.

100. Stadler Group. *Variobahn Low-Floor Light Rail Vehicle*; Stadler Group: Aarhus, Denmark, 2016.

101. Brookville Corp. *Liberty Modern Streetcars*; Brookville Corp: Brookville, PA, USA, 2012.

102. Transport Assets Standards Authority. *Traction Power Supply Infrastructure and Light Rail Vehicle Interface T LR EL 00007 ST*; Transport Asset Standards Authority: Sydney, NSW, Australia, 2018.

103. Su, Y.-G.; Xie, S.-Y.; Hu, A.P.; Tang, C.-S.; Zhou, W.; Huang, L. Capacitive Power Transfer System with a Mixed-Resonant Topology for Constant-Current Multiple-Pickup Applications. *IEEE Trans. Power Electron.* **2017**, *32*, 8778–8786. [CrossRef]

104. Chopra, S.; Bauer, P. Driving Range Extension of EV With On-Road Contactless Power Transfer—A Case Study. *IEEE Trans. Ind. Electron.* **2011**, *60*, 329–338. [CrossRef]

105. Dai, J.; Ludois, D.C. Capacitive Power Transfer Through a Conformal Bumper for Electric Vehicle Charging. *IEEE J. Emerg. Sel. Top. Power Electron.* **2016**, *4*, 1015–1025. [CrossRef]

106. Adamowicz, M.; Szewczyk, J. SiC-Based Power Electronic Traction Transformer (PETT) for 3 kV DC Rail Traction. *Energies* **2020**, *13*, 5573. [CrossRef]

107. Alstom. Alstom Presents APS for Road, Its Innovative Electric Road Solution, Alstom, 11 November 2017. Available online: https://www.alstom.com/press-releases-news/2017/11/alstom-presents-aps-for-road-its-innovative-electric-road-solution (accessed on 28 March 2022).

108. Yi, Z.; Chen, Z.; Yin, K. Sensing as the key to the safety and sustainability of new energy storage devices. *Prot. Control Mod. Power Syst.* **2023**, *8*, 1–22. [CrossRef]

109. Zhang, M.; Yang, D.; Du, J.; Sun, H.; Li, L.; Wang, L.; Wang, K. A Review of SOH Prediction of Li-Ion Batteries Based on Data-Driven Algorithms. *Energies* **2022**, *16*, 3167. [CrossRef]